

The spin-resolved atomic velocity distribution and 21-cm line profile of dark-age gas

Christopher M. Hirata^{*} and Kris Sigurdson^{*†}

Institute for Advanced Study, Einstein Drive, Princeton, NJ 08540, USA

21 September 2018

ABSTRACT

The 21-cm hyperfine line of atomic hydrogen (HI) is a promising probe of the cosmic dark ages. In past treatments of 21-cm radiation it was assumed the hyperfine level populations of HI could be characterized by a velocity-independent “spin temperature” T_s determined by a competition between 21-cm radiative transitions, spin-changing collisions, and (at lower redshifts) Ly α scattering. However we show here that, if the collisional time is comparable to the radiative time, the spin temperature will depend on atomic velocity, $T_s = T_s(v)$, and one must replace the usual hyperfine level rate equations with a Boltzmann equation describing the spin and velocity dependence of the HI distribution function. We construct here the Boltzmann equation relevant to the cosmic dark ages and solve it using a basis-function method. Accounting for the actual spin-resolved atomic velocity distribution results in up to a ~ 2 per cent suppression of the 21-cm emissivity, and a redshift and angular-projection dependent suppression or enhancement of the linear power spectrum of 21-cm fluctuations of up to ~ 5 per cent. The effect on the 21-cm line profile is more dramatic — its full-width at half maximum (FWHM) can be enhanced by up to ~ 60 per cent relative to the velocity-independent calculation. We discuss the implications for 21-cm tomography of the dark ages.

Key words: cosmology: theory – intergalactic medium – atomic processes – line: profiles.

1 INTRODUCTION

While both earlier and later epochs of the Universe have now been observed by astronomers, the cosmic dark ages (the time between the formation of the first atoms at $z \sim 1000$ and the subsequent formation of the first luminous objects) remain an observational enigma. The difficulty of probing this epoch stems from the relatively inert physical properties expected of the dark-age gas. It is diffuse, without the luminous galaxies or quasars that have proven so useful for lower-redshift astrophysics. It is mostly neutral, hence signatures such as recombination lines, free-free radiation, and Compton scattering of the cosmic microwave background (CMB) are essentially absent. Finally, its composition consists mainly of cold H and He atoms, which have very few lines that can be excited at the relevant temperatures.

A notable exception to this last property is the hyperfine 21-cm line of neutral hydrogen (HI). The HI 21-cm line has attracted considerable attention as a possible probe of cosmic evolution during the dark ages, despite substantial observational challenges. In particular by using frequency as well as angular information, it should be possible to map out the 21-cm signal in three dimensions, thereby greatly increasing the number of modes that can be observed (Loeb & Zaldarriaga 2004; Morales et al. 2005; Bowman et al. 2005). Furthermore, the foregrounds to this signal are expected to have a distinctly different character in both angular and especially frequency space (they are expected to be relatively smooth in frequency space) which should allow for effective foreground removal (Zaldarriaga et al. 2004; Santos et al. 2005; Wang et al. 2005).

The nature of the 21-cm signal depends on both the properties of the primordial gas and the mechanisms that excite

^{*} E-mail: chirata@sns.ias.edu (CMH); krs@sns.ias.edu (KS)

[†] Hubble Fellow

or de-excite the hydrogen atoms. The major mechanisms operating during the dark ages are the radiative transitions at $\lambda_{21} = 21.1$ cm and atom-atom collisions; the former tend to cause the hyperfine level populations to relax to the CMB temperature T_γ , whereas the latter tend to drive the level populations towards the gas kinetic temperature T_k . The atomic gas is expected to be colder than the CMB during the dark ages since it cools adiabatically as $T \propto a^{-2}$ after residual Compton heating becomes ineffective. During this period we thus expect to see the 21-cm signal in absorption when the collisional coupling is strong and Loeb & Zaldarriaga (2004) have shown that at high redshifts $z \geq 50$ the entire Universe should be collisionally coupled and an absorption signal should be present. At lower redshifts collisions become less efficient due to the low density and the level populations approach T_γ ; in this case the absorption signal fades because the H I spins are nearly in thermal equilibrium with the CMB. Only the highest-density regions remain collisionally coupled, and these may even appear in emission if shocks or adiabatic compression heat them to $T_k > T_\gamma$ (Iliev et al. 2002, 2003). At later times when sources of ultraviolet radiation have turned on, scattering of photons in the H I Ly α resonance can also become significant, and can once again drive the level populations towards T_k even in mean-density and underdense regions. These early sources of radiation may also have emitted X-rays, which could heat the intergalactic medium (IGM) to well above the CMB temperature (Madau et al. 1997; Chen & Miralda-Escudé 2004; Kuhlen & Madau 2005), and perhaps produce sufficient ionization that atom-electron collisions are important in determining the spin temperature in some regions (Kuhlen et al. 2006).

A detailed understanding of all these excitation and de-excitation mechanisms and their effect on the 21-cm emissivity and line profile will be necessary in order to interpret future 21-cm observations. In the 1950s and 1960s, analysis of 21-cm radiation from the interstellar medium motivated pioneering studies of the Ly α scattering (Wouthuysen 1952; Field 1958, 1959) and collisional (Dalgarno 1961; Allison & Dalgarno 1969) mechanisms. The results of these analyses have largely been carried over into the theory of 21-cm radiation from the high-redshift IGM and dark ages, with some improvements and adaptations to accommodate different physical situations. For example, several authors have computed the efficiency of the Ly α scattering mechanism with detailed consideration of cosmological radiative transfer effects, interaction with Ly β and higher-order H I Lyman lines, and the fine and hyperfine structure of the Ly α resonance (Chen & Miralda-Escudé 2004; Hirata 2006; Pritchard & Furlanetto 2006; Chuzhoy & Shapiro 2005). Zygelman (2005) has also re-evaluated the collisional hyperfine excitation rate using modern atomic physics techniques.

In this paper we note that heretofore all studies of high-redshift 21-cm radiation have assumed that the hyperfine level population ratios of the hydrogen atoms in the primordial gas are independent of velocity. If the level populations are also isotropic, they depend only on the total spin F and not on the magnetic quantum number M_F , so they can be characterized by a single spin temperature T_s .¹ This assumption implies that the ratio of hyperfine level populations is $n_{\text{HI}}(F=1)/n_{\text{HI}}(F=0) \equiv 3e^{-T_\star/T_s}$ independent of the velocity of the hydrogen atoms.² This should be the case if the level populations are determined solely by radiative transitions with the CMB in the 21-cm line or solely by atomic collisions as, in these cases, the hyperfine level populations will thermalize at a temperature T_γ or T_k respectively. However we demonstrate here that, because the level populations are determined by both radiative and collisional transitions and the collisional spin-change cross section for H-H collisions is velocity dependent while the radiative cross section is velocity independent, *the hyperfine level-resolved distribution function of H I is not thermal*. This is our main result and we show below that this has a significant (order unity) effect on the 21-cm line profile of collisionally coupled gas at high redshift.

The paper is organized as follows: We outline the basic kinetic theory and derive the collisional piece of the linear Boltzmann equation in Section 2 and define the basis-function method we use to describe deviations from a thermal distribution function in Section 3. In Section 4 we evaluate the H-H collision term and in Section 5 we evaluate the He-H collision term to account for the effects of helium. We solve the Boltzmann equation in Section 6 and present our results for the 21-cm line profile in Section 7. A short discussion and summary of our main results follows in Section 8. We have included in Appendix A a summary of some useful properties of the Gauss-Hermite basis functions, and in Appendix B the details of the quantum mechanical calculation of the relevant atomic cross sections. When needed for our numerical results we have assumed a flat cosmology with matter density $\Omega_m = 0.30$, baryon density $\Omega_b = 0.042$, Hubble constant $H_0 = 72 \text{ km s}^{-1} \text{ Mpc}^{-1}$, primordial helium fraction $Y_{\text{He}} = 0.24$, and CMB temperature $T_0 = 2.728 \text{ K}$.

2 KINETIC THEORY

In the standard calculation of the 21-cm signal one uses the populations $n_{\text{HI}}(F=0)$ and $n_{\text{HI}}(F=1)$ of the ground and hyperfine-excited levels as the basic quantities which describe the state of the hydrogen atoms. In this paper we aim to go

¹ Several groups have discussed the possibility of M_F -dependent populations due to magnetic fields (Cooray & Furlanetto 2005), CMB anisotropy (Zygelman 2005), and anisotropies in the Ly α radiation (Babich & Loeb 2005). In all cases the effect was argued to be very small, and indeed Zygelman (2005) showed that if any net spin polarization of the H I atoms was initially present, it would be destroyed by radiative transitions much faster than the Hubble time.

² Here $T_\star \equiv hc/\lambda_{21}k_B = 68.2 \text{ mK}$ is the energy of the 21-cm transition in temperature units.

beyond this calculation by solving for the joint distribution of spins and velocities. This will be represented by the distribution function, $f_F(\mathbf{v})$, which describes the number of atoms in hyperfine level F per unit volume in position space, per unit volume in velocity space. For comparison, the standard calculation assumes that the distribution function can be separated into its kinetic degrees of freedom with temperature T_k and its spin degrees of freedom with temperature T_s . In this case one can write

$$f_F(\mathbf{v})|_{T_s} = n_{\text{HI}} y_F \Phi_{T_k}(\mathbf{v}), \quad (1)$$

where $\Phi_{T_k}(\mathbf{v})$ represents the Maxwellian distribution,

$$\Phi_{T_k}(\mathbf{v}) = \frac{1}{(2\pi\sigma^2)^{3/2}} e^{-v^2/2\sigma^2}, \quad (2)$$

$\sigma = \sqrt{k_B T_k / m_{\text{H}}}$ is the thermal velocity dispersion of the atoms, and \mathbf{v} is the velocity of the atom in the reference frame of the baryonic fluid. Note that here and elsewhere in the paper the notation “ $|_{T_s}$ ” is shorthand for “evaluated in the spin-temperature approximation.” The factor y_F in Eq. (1) is the fraction of the atoms in the F hyperfine level, and an elementary calculation shows that this quantity is related to the spin temperature by

$$y_0 = \frac{1}{3e^{-T_\star/T_s} + 1} \approx \frac{1}{4} + \frac{3T_\star}{16T_s} \quad \text{and} \quad y_1 = \frac{3e^{-T_\star/T_s}}{3e^{-T_\star/T_s} + 1} \approx \frac{3}{4} - \frac{3T_\star}{16T_s}, \quad (3)$$

where the approximation $T_\star \ll T_s$ is valid in all cases of astrophysical interest. The standard analysis solves for T_s using the continuity equation for $F = 0$ and $F = 1$ HI atoms. By determining all rates (collisional, radiative, and Ly α) of production or destruction of HI atoms in a given level one obtains the abundances $n(F)$ and hence the spin temperature $e^{-T_\star/T_s} = n(1)/[3n(0)]$. In the standard case, the brightness temperature due to the 21-cm line is

$$T_b|_{T_s} = \left[\frac{H(z)}{1+z} + \frac{dv_{\parallel}^{\text{(pec)}}}{dr_{\parallel}} \right]^{-1} \frac{3c^3 AT_\star}{32\pi\nu_{10}^3(1+z)^2} n_{\text{HI}} \left(1 - \frac{T_\gamma}{T_s} \right), \quad (4)$$

where $H(z)$ is the Hubble rate, $v_{\parallel}^{\text{(pec)}}$ is the radial component of the peculiar velocity, c is the speed of light, A is the 21-cm Einstein coefficient, ν_{10} is the frequency of the 21-cm line, and T_γ is the CMB temperature (Bharadwaj & Ali 2004; Barkana & Loeb 2005). One of the major goals of this paper is to update Eq. (4) to include the full spin-velocity distribution.

2.1 Simplifying approximations; distribution function

The distribution function $f_F(\mathbf{v})$ is a much more general description of the state of the gas than the three numbers $\{n_{\text{HI}}, T_k, T_s\}$ in the standard treatment. Nevertheless, the most general description possible would also account for dependence on M_F and quantum correlations among the various states of HI. In this section we describe the key simplifying approximations that allow us to fully characterize the HI atoms by a distribution function.

Since the spin state of a hydrogen atom is described by its two quantum numbers $|FM_F\rangle$, the most general characterization would be to write a quantum-mechanical density matrix $\rho_{FM_F, F'M'_F}(\mathbf{r}, \mathbf{v})$, so that e.g. $\rho_{00,00}(\mathbf{r}, \mathbf{v})$ would describe the number of H atoms in the ground state per unit volume, per unit volume in velocity space. The use of the density matrix allows for correlations between states of different F or M_F , just as the U and V Stokes parameters allow for correlations between the horizontal and vertical polarizations of light in radiative transfer theory. In the realistic high-redshift Universe, we do not expect correlations between states with $F = 0$ and states with $F = 1$, because their energy splitting implies any such correlations are destroyed on a timescale of $h/\Delta E \sim 10^{-9}$ s much shorter than the collisional or radiative transition timescale. There may however be correlations between states with $F = 1$ but different M_F , since these are degenerate (except for small effects such as Zeeman splitting; Cooray & Furlanetto 2005).

This general problem can be simplified considerably for the special case where (A) the spin and velocity relaxation times are fast compared to the diffusion or free-streaming time across scales where bulk velocity or temperature gradients are significant; (B) the spin and velocity relaxation times are fast compared to the expansion, rotation, and shearing timescales of the fluid, and the Hubble and Compton-heating timescales; (C) an isotropic radiation field with smooth frequency dependence (such as the CMB); and (D) collisional transitions are dominated by spin exchange mechanisms. These are very good approximations in most of the Universe (i.e. regions of near mean density) during the dark ages. In these regions, the spin relaxation time, considering radiative transitions alone, is $T_\star/4AT_\gamma = 2[40/(1+z)]$ kyr, which is much faster than the Hubble time, $100[40/(1+z)]^{3/2}$ Myr (note that collisions at high redshift act to decrease the spin relaxation time.) The velocity relaxation time, i.e. the timescale for the H atoms to relax to a Maxwellian distribution, is 120 kyr at $1+z = 40$.³ In regions of near mean density, the expansion time is of order the Hubble time, and the rotation and shearing timescales are longer; thus condition

³ The number given here is the inverse decay constant of the slowest-decaying perturbation from a Maxwellian distribution. Technically, it is computed as the inverse of the smallest positive eigenvalue of $X'_{\Sigma\Sigma}$ defined in Eq. (71).

(B) should be valid. Prior to collapse the expectation is that the velocity and temperature are smooth on scales smaller than the Jeans length; since the Jeans length is roughly the distance an atom can travel in a Hubble time (neglecting collisions), it follows that if (B) is valid, then (A) should be valid in either the diffusion or free-streaming cases. The CMB is isotropic and has blackbody frequency dependence, so (C) should be valid unless the 21-cm radiation adds (or subtracts) significantly to (or from) the CMB temperature. The mean 21-cm brightness temperature from high-redshift gas has been computed to be < 1 per cent of the CMB temperature (e.g. Loeb & Zaldarriaga 2004), so (C) should be valid in regions of order mean density. Finally, the ratio of dipolar relaxation to spin exchange rate is of order 10^{-2} or less at all relevant temperatures (Zygelman 2005), so (D) is valid.

The simplifications allowed by (A–D) are as follows. Condition (A) implies that the problem of solving for the density matrix and associated master equation can be solved locally, eliminating the position \mathbf{r} from the problem. Condition (B) implies that we can treat the determination of the distribution function within the steady-state approximation, rather than evolving the Boltzmann equation from the recombination epoch forward to the epoch of interest. Condition (C) implies that the radiative transition rates are independent of the magnitude and direction of the atom’s velocity and are isotropic (i.e. no value of M_F is favoured); the smoothness of the frequency dependence is important because otherwise it would be possible for atoms moving in different directions to have different 21-cm excitation rates due to the Doppler shift. Condition (D) further implies that there is no coupling between the direction of spins and the direction of velocities. Thus in addition to being isotropic under rotations of both velocities and spins together, the problem is isotropic under rotations of velocities and spins separately. Therefore once a steady-state solution is reached, one can assume that the density matrix $\rho_{FM_F, F'M'_F}(\mathbf{v})$ is isotropic under rotations of the spins, i.e. it takes the form

$$\rho_{FM_F, F'M'_F}(\mathbf{v}) = \begin{pmatrix} f_0(\mathbf{v}) & 0 & 0 & 0 \\ 0 & f_1(\mathbf{v})/3 & 0 & 0 \\ 0 & 0 & f_1(\mathbf{v})/3 & 0 \\ 0 & 0 & 0 & f_1(\mathbf{v})/3 \end{pmatrix} \quad (5)$$

in the $\{|00\rangle, |1-1\rangle, |10\rangle, |11\rangle\}$ basis. Here $f_F(\mathbf{v})$ is the level-resolved distribution function, and it represents the number of hydrogen atoms in the hyperfine level with total spin $F \in \{0, 1\}$ per unit volume in physical space, per unit volume in velocity space. The total number density of hydrogen atoms is simply

$$n_{\text{HI}} = \sum_{F=0}^1 \int f_F(\mathbf{v}) d^3\mathbf{v}. \quad (6)$$

The key problem solved in this paper is to determine the distribution function $f_F(\mathbf{v})$ under the above-described conditions (A–D) by constructing the Boltzmann equation and finding its steady-state solution, and the associated 21-cm emission. Computationally, this is a significant simplification as compared to solving for $\rho_{FM_F, F'M'_F}(\mathbf{r}, \mathbf{v})$. The limitations of this approach should be kept in mind however. The most serious limitation is condition (C), which can be violated if the 21-cm line radiation ever becomes comparable in intensity to the CMB (i.e. if the line brightness temperature becomes $\sim T_\gamma$). This does not occur in regions of the Universe near mean density, but it may happen in minihaloes (e.g. Shapiro et al. 2005) and thus our results should be used with caution in this case.

2.2 Evolution equations

The distribution function evolves according to several effects including radiative transitions, collisions with various species, Lyman- α scattering, and bulk velocity gradients. In general one can decompose the rate of change of the distribution function into these effects as

$$\dot{f}_F(\mathbf{v}) = \dot{f}_F^{(\text{rad})}(\mathbf{v}) + \dot{f}_F^{(\text{col}, \text{H-H})}(\mathbf{v}) + \dot{f}_F^{(\text{col}, \text{H-He})}(\mathbf{v}) + \dot{f}_F^{(\text{col}, \text{H-e}^-)}(\mathbf{v}) + \dot{f}_F^{(\text{col}, \text{H-H}^+)}(\mathbf{v}) + \dot{f}_F^{(\text{Ly}\alpha)}(\mathbf{v}) + \dot{f}_F^{(\mathbf{v}_b)}(\mathbf{v}). \quad (7)$$

The term associated with the bulk baryonic fluid velocity \mathbf{v}_b is,

$$\dot{f}_F^{(\mathbf{v}_b)}(\mathbf{v}) = a^{-1} v^i \frac{\partial (v_b)^j}{\partial r^i} \frac{\partial f_F(\mathbf{v})}{\partial v^j}, \quad (8)$$

because the velocity \mathbf{v} of the atom relative to the baryonic fluid changes as the atom moves to a region of different \mathbf{v}_b even if there are no forces acting on the atom. (The Hubble expansion is considered to be part of the velocity gradient.) We neglect this term since the associated timescale is of order the Hubble timescale (in mean-density regions) or the collapse timescale (in collapsing regions), either of which is long compared to the spin-relaxation timescale.

Of the remaining terms, the radiative transition term is the simplest to compute. The photon phase space density in the 21-cm line is given by the blackbody formula $\mathcal{N} = (e^{T_\gamma/T_\gamma} - 1)^{-1}$. We neglect the change in momentum of the atom due to absorption or emission of a 21-cm photon, which is an excellent approximation since the recoil energy in temperature units is $(h\nu_{10}/c)^2/2k_B m_{\text{H}} = 2 \times 10^{-16}$ K. Then the radiative term becomes

$$\dot{f}_1^{(\text{rad})}(\mathbf{v}) = -\dot{f}_0^{(\text{rad})}(\mathbf{v}) = -A(1 + \mathcal{N})f_1(\mathbf{v}) + 3ANf_0(\mathbf{v}). \quad (9)$$

The collisional term is more complicated. For the case of H-H collisions, we have

$$\begin{aligned} \dot{f}_F^{(\text{col,H-H})}(\mathbf{v}) &= -\sum_{F'=0}^1 \int K_{FF'}(\mathbf{v}' - \mathbf{v}) f_F(\mathbf{v}) f_{F'}(\mathbf{v}') d^3\mathbf{v}' \\ &\quad + \frac{1}{2} \sum_{F',F''} \int K_{F'F''}(\mathbf{v}'' - \mathbf{v}') f_{F'}(\mathbf{v}') f_{F''}(\mathbf{v}'') p_{F|F'F''}(\mathbf{v}|\mathbf{v}', \mathbf{v}'') d^3\mathbf{v}' d^3\mathbf{v}''. \end{aligned} \quad (10)$$

Here $K_{F'F''}$ is the product of cross section and relative velocity for two hydrogen atoms in the F' and F'' level, and $p_{F|F'F''}(\mathbf{v}|\mathbf{v}', \mathbf{v}'')$ is the probability density for such a collision to produce a final-state H atom in the F level with velocity \mathbf{v} . The factor of 1/2 in the second term avoids double-counting of collisions since the integral over $d^3\mathbf{v}' d^3\mathbf{v}''$ extends over all of \mathbb{R}^6 . The probability $p_{F|F'F''}(\mathbf{v}|\mathbf{v}', \mathbf{v}'')$ must integrate to 2 since the final state has two H atoms:

$$\sum_{F=0}^1 \int p_{F|F'F''}(\mathbf{v}|\mathbf{v}', \mathbf{v}'') d^3\mathbf{v} = 2. \quad (11)$$

A similar but simpler collision term applies for H-He, H-H⁺, and H-e⁻ collisions, but of course in these cases Eq. (11) integrates to 1, and there is no summation over hyperfine levels of the target (i.e. the F' summation in Eq. 10 is not needed). Since He is a spin singlet, spin exchange does not occur in H-He collisions, however in general $\dot{f}_F^{(\text{col,H-He})}(\mathbf{v}) \neq 0$ because the collision changes the velocity of the H atom. For this reason we have included helium, but its effects turn out to be small (< 0.1 per cent in the line FWHM and total emissivity). Note that while the direct effect of He collisions is small the 21-cm emissivity still depends on the He fraction Y_{He} because it sets the density of H atoms and the evolution of T_k .

In this paper we will neglect the atom-electron and atom-proton collision terms as we are interested in the period before UV or X-ray sources become important and begin to produce ionization. There are some free electrons and protons (abundance $x_e \approx 2 \times 10^{-4}$; Seager et al. 1999) during the Dark Ages since the cosmological recombination does not run to completion. A rough estimate of the importance of the electrons can be obtained by the previously computed thermal-averaged spin-change ($F = 1 \rightarrow 0$) cross sections $\langle \sigma_{10v} \rangle$; using the values of the H-H cross section in Zygelman (2005) and the H-e⁻ cross section of Smith (1966a), we find $x_e \langle \sigma_{10v} \rangle_{\text{H-e}^-} / \langle \sigma_{10v} \rangle_{\text{H-H}} \simeq 0.01$ at $T_k = 10 \text{ K}$ ($z = 21$) and less at higher redshifts. We thus conclude that electrons change the collisional spin-change rate at the sub per cent level during the epoch of interest. The spin-change rate due to collisions with protons is even smaller (Smith 1966a).

2.3 Perturbation theory

In general the evolution equations are nonlinear and solving them is highly nontrivial. However, in the cases of interest, $T_\star = 68.2 \text{ mK}$ is much less than either T_k or T_γ and the equations can be linearized by expanding around the thermal equilibrium solution. We define

$$f_F^{(\text{th})}(\mathbf{v}) = n_{\text{HI}} y_F(T_k) \Phi_{T_k}(\mathbf{v}). \quad (12)$$

to be the thermal distribution function at temperature T_k .⁴ We can now define the perturbation

$$\xi_F(\mathbf{v}) = f_F(\mathbf{v}) - f_F^{(\text{th})}(\mathbf{v}). \quad (13)$$

Since $f_F^{(\text{th})}(\mathbf{v})$ is a constant, all of the evolution equations can be trivially expressed in terms of $\xi_F(\mathbf{v})$ and its time derivative. In terms of these new variables the radiative transition term becomes

$$\dot{\xi}_1^{(\text{rad})}(\mathbf{v}) = A \frac{-3e^{-T_\star/T_k}(1 + \mathcal{N}) + 3\mathcal{N}}{3e^{-T_\star/T_k} + 1} n_{\text{HI}} \Phi_{T_k}(\mathbf{v}) - A(1 + \mathcal{N})\xi_1(\mathbf{v}) + 3AN\xi_0(\mathbf{v}), \quad (14)$$

and working to lowest order in T_\star this simplifies to

$$\dot{\xi}_1^{(\text{rad})}(\mathbf{v}) = \frac{3}{4} A \left(\frac{T_\gamma}{T_k} - 1 \right) n_{\text{HI}} \Phi_{T_k}(\mathbf{v}) - \frac{T_\gamma}{T_\star} A [\xi_1(\mathbf{v}) - 3\xi_0(\mathbf{v})]. \quad (15)$$

The equation for the $F = 0$ levels is related to this by $\dot{\xi}_0^{(\text{rad})}(\mathbf{v}) = -\dot{\xi}_1^{(\text{rad})}(\mathbf{v})$.

The H-H collisional term in the evolution equation is evaluated by substituting Eq. (13) into Eq. (10) and expanding to leading order in ξ . In principle, the collision term includes zeroth, first, and second-order terms. However, the zeroth-order terms vanish because if the velocities and spin level populations were thermal then the distribution function would be

⁴ Note that $f_F^{(\text{th})}(\mathbf{v})$ is computed with the spins thermalized at T_k .

independent of time. The remaining terms are

$$\begin{aligned} \dot{\xi}_F^{(\text{col,H-H})}(\mathbf{v}) &= - \sum_{F'=0}^1 \int K_{FF'}(\mathbf{v}' - \mathbf{v}) \xi_F(\mathbf{v}) f_{F'}^{(\text{th})}(\mathbf{v}') d^3 \mathbf{v}' - \sum_{F'=0}^1 \int K_{FF'}(\mathbf{v}' - \mathbf{v}) f_F^{(\text{th})}(\mathbf{v}) \xi_{F'}(\mathbf{v}') d^3 \mathbf{v}' \\ &+ \sum_{F',F''} \int K_{F'F''}(\mathbf{v}'' - \mathbf{v}') \xi_{F'}(\mathbf{v}') f_{F''}^{(\text{th})}(\mathbf{v}'') p_{F|F'F''}(\mathbf{v}|\mathbf{v}',\mathbf{v}'') d^3 \mathbf{v}' d^3 \mathbf{v}'' \\ &+ \sum_{F',F''} \int K_{F'F''}(\mathbf{v}'' - \mathbf{v}') \xi_{F'}(\mathbf{v}') \xi_{F''}(\mathbf{v}'') p_{F|F'F''}(\mathbf{v}|\mathbf{v}',\mathbf{v}'') d^3 \mathbf{v}' d^3 \mathbf{v}'' \end{aligned} \quad (16)$$

So long as the kinetic and radiation temperatures are $\gg T_*$, we will have $|\xi_F(\mathbf{v})| \ll f_F^{(\text{th})}(\mathbf{v})$ and the second-order term on the last line of this equation can be neglected.

3 BASIS FUNCTION METHOD

It is convenient at this point to expand the perturbation variable in a basis set. We write

$$\xi_F(\mathbf{v}) = \sum_n \xi_{Fn} \phi_n(\mathbf{v}), \quad (17)$$

where $\phi_n(\mathbf{v})$ form a set of basis functions satisfying the orthonormality relation,

$$\int \phi_n^*(\mathbf{v}) \phi_{n'}(\mathbf{v}) d^3 \mathbf{v} = \left(\frac{m_{\text{H}}}{4\pi k_B T_k} \right)^{3/2} \delta_{nn'}. \quad (18)$$

The normalization has been chosen so that the thermal distribution is one of the basis modes: $\phi_0(\mathbf{v}) = \Phi_{T_k}(\mathbf{v})$. The remaining modes are chosen to be the Gaussian-weighted Hermite polynomials,

$$\phi_n(\mathbf{v}) = 2^{-n-5/2} \pi^{-3/2} [(2n+1)!]^{-1/2} \frac{1}{\sigma^2 v} H_{2n+1} \left(\frac{v}{\sigma} \right) e^{-v^2/2\sigma^2}, \quad (19)$$

which indeed satisfy Eq. (18). The $\{\phi_n\}_{n=0}^{\infty}$ are complete only for spherically symmetric functions (functions that depend only on the magnitude v) and in general additional basis functions with angular dependence must be included. However, since our problem is spherically symmetric, there is no need to include them.

Written in terms of basis functions Eq. (15) becomes

$$\dot{\xi}_{1n}^{(\text{rad})} = \frac{3}{4} A \left(\frac{T_\gamma}{T_k} - 1 \right) n_{\text{HI}} \delta_{n,0} - \frac{T_\gamma}{T_*} A (\xi_{1n} - 3\xi_{0n}), \quad (20)$$

and $\dot{\xi}_{0n}^{(\text{rad})} = -\dot{\xi}_{1n}^{(\text{rad})}$. Evaluation of the collisional rates is aided by defining several integrals. We define for the H-H collisions,

$$\begin{aligned} X_{F_n, F'_{n'}}^{(\text{col,H-H})} &= (4\pi\sigma^2)^{3/2} \left[\int \sum_{F''} y_{F''}(T_k) K_{F'F''}(\mathbf{v}'' - \mathbf{v}) \phi_n(\mathbf{v}) \phi_{n'}(\mathbf{v}') \phi_0(\mathbf{v}'') d^3 \mathbf{v} d^3 \mathbf{v}'' \right. \\ &+ \int y_F(T_k) K_{FF'}(\mathbf{v} - \mathbf{v}') \phi_n(\mathbf{v}) \phi_{n'}(\mathbf{v}') \phi_0(\mathbf{v}) d^3 \mathbf{v} d^3 \mathbf{v}' \\ &\left. - \int \sum_{F''} y_{F''}(T_k) K_{F'F''}(\mathbf{v}'' - \mathbf{v}') p_{F|F'F''}(\mathbf{v}|\mathbf{v}',\mathbf{v}'') \phi_n(\mathbf{v}) \phi_{n'}(\mathbf{v}') \phi_0(\mathbf{v}'') d^3 \mathbf{v} d^3 \mathbf{v}' d^3 \mathbf{v}'' \right]. \end{aligned} \quad (21)$$

The first-order terms in Eq. (16) then can be written compactly as

$$\dot{\xi}_{Fn}^{(\text{col,H-H})} = -n_{\text{HI}} \sum_{F'} X_{F_n, F'_{n'}}^{(\text{col,H-H})} \xi_{F'n'}. \quad (22)$$

Before proceeding, we note that the Maxwellian velocity distribution of Eq. (1) assumed in the standard calculation corresponds to a perturbation

$$\xi_F(\mathbf{v})|_{T_s} = [y_F(T_s) - y_F(T_k)] n_{\text{HI}} \Phi_{T_k}(\mathbf{v}) = \frac{3T_*}{16} (-1)^F (T_s^{-1} - T_k^{-1}) n_{\text{HI}} \Phi_{T_k}(\mathbf{v}), \quad (23)$$

or equivalently

$$\xi_{Fn}|_{T_s} = \frac{3T_*}{16} (-1)^F (T_s^{-1} - T_k^{-1}) n_{\text{HI}} \delta_{n,0}. \quad (24)$$

In this case only the lowest basis mode ($n = 0$) is excited. In the full calculation, we will find that in general ξ_{Fn} can be nonzero for any value of n .

4 EVALUATION OF H-H COLLISION TERM

4.1 The relation of K and p to the cross section

Our objective here is to compute $K_{F'F''}(\mathbf{v}'' - \mathbf{v}')$ and $p_{F|F'F''}(\mathbf{v}|\mathbf{v}', \mathbf{v}'')$. These are related to the differential cross section as follows. Defining

$$\mathbf{u} = \frac{\mathbf{v}'' + \mathbf{v}'}{2} \quad \text{and} \quad \mathbf{w} = \mathbf{v}'' - \mathbf{v}', \quad (25)$$

we find that

$$K_{F'F''}(\mathbf{v}'' - \mathbf{v}') = w \sigma_{F'F''}(w). \quad (26)$$

The probability distribution for scattered products is

$$p_{F|F'F''}(\mathbf{v}|\mathbf{v}', \mathbf{v}'') d^3 \mathbf{v} = \frac{dP_{F|F'F''}}{d\hat{\Omega}} d^2 \hat{\Omega}, \quad (27)$$

where $dP_{F|F'F''}/d\hat{\Omega}$ is the joint probability distribution for the final outgoing angle $\hat{\Omega}$ and spin F (which in general depends on the angle between $\hat{\Omega}$ and $\hat{\mathbf{w}}$) and

$$\mathbf{v} = \mathbf{u} + \frac{1}{2} w \hat{\Omega}. \quad (28)$$

The final relative velocity is w within the approximation of elastic scattering (valid when $T_* \ll T_k$) where we neglect the hyperfine energy defect in comparison with the kinetic energy. Note once again that the joint probability distribution integrates to 2 because there are 2 H atoms:

$$\sum_{F=0}^1 \int \frac{dP_{F|F'F''}}{d\hat{\Omega}} d^2 \hat{\Omega} = 2. \quad (29)$$

The explicit expressions for the differential cross section can be derived by techniques described in e.g. Smith (1966b) and are summarized in Appendix B for reference.

4.2 Evaluation of integrals

We focus our attention on the third integral appearing in brackets in Eq. (21):

$$\mathcal{I} = \int \sum_{F''} y_{F''}(T_k) K_{F'F''}(\mathbf{v}'' - \mathbf{v}') p_{F|F'F''}(\mathbf{v}|\mathbf{v}', \mathbf{v}'') \phi_n(\mathbf{v}) \phi_{n'}(\mathbf{v}') \phi_0(\mathbf{v}'') d^3 \mathbf{v} d^3 \mathbf{v}' d^3 \mathbf{v}''. \quad (30)$$

If we can evaluate this integral the first two integrals can also be evaluated by replacing $p_{F|F'F''}(\mathbf{v}|\mathbf{v}', \mathbf{v}'')$ with $\delta_{FF'} \delta^{(3)}(\mathbf{v} - \mathbf{v}'')$ or $\delta_{FF''} \delta^{(3)}(\mathbf{v} - \mathbf{v}')$ respectively. In terms of the differential cross sections of §4.1 this corresponds to setting $dP_{F|F'F''}/d\hat{\Omega}$ equal to $\delta_{FF'} \delta^{(2)}(\hat{\Omega} + \hat{\mathbf{w}})$ or $\delta_{FF''} \delta^{(2)}(\hat{\Omega} - \hat{\mathbf{w}})$ respectively.

Upon substituting Eq. (27) into \mathcal{I} , we get

$$\mathcal{I} = \int \sum_{F''} y_{F''}(T_k) K_{F'F''}(w) \frac{dP_{F|F'F''}}{d\hat{\Omega}} \phi_n \left(\mathbf{u} + \frac{1}{2} w \hat{\Omega} \right) \phi_{n'} \left(\mathbf{u} - \frac{1}{2} w \hat{\Omega} \right) \phi_0 \left(\mathbf{u} + \frac{1}{2} w \hat{\Omega} \right) d^3 \mathbf{u} d^3 \mathbf{w} d^2 \hat{\Omega}. \quad (31)$$

Since we are considering only the spherically symmetric modes ϕ_n this integral can be simplified by symmetry considerations. We first split the integration over \mathbf{w} into integrals over magnitude w and direction $\hat{\mathbf{w}}$: $d^3 \mathbf{w} = w^2 dw d\hat{\mathbf{w}}$. If we then evaluate the $d^3 \mathbf{u} dw d^2 \hat{\Omega}$ integral the result must be independent of the direction of $\hat{\mathbf{w}}$. We can thus replace $\hat{\mathbf{w}}$ with any unit vector, say the unit vector in the third coordinate direction \mathbf{e}_3 . This gives

$$\mathcal{I} = 4\pi \int \sum_{F''} y_{F''}(T_k) K_{F'F''}(w) \frac{dP_{F|F'F''}}{d\hat{\Omega}} \phi_n \left(\mathbf{u} + \frac{1}{2} w \hat{\Omega} \right) \phi_{n'} \left(\mathbf{u} - \frac{1}{2} w \mathbf{e}_3 \right) \phi_0 \left(\mathbf{u} + \frac{1}{2} w \mathbf{e}_3 \right) w^2 d^3 \mathbf{u} dw d^2 \hat{\Omega}. \quad (32)$$

By a similar argument if we decompose $\hat{\Omega}$ into spherical coordinates,

$$\hat{\Omega} = \cos \theta \mathbf{e}_3 + \sin \theta (\cos \varphi \mathbf{e}_1 + \sin \varphi \mathbf{e}_2), \quad (33)$$

then φ can be integrated out to yield

$$\begin{aligned} \mathcal{I} &= 8\pi^2 \int \sum_{F''} y_{F''}(T_k) K_{F'F''}(w) \frac{dP_{F|F'F''}}{d\hat{\Omega}} \phi_n \left[\mathbf{u} + \frac{w}{2} (\cos \theta \mathbf{e}_3 + \sin \theta \mathbf{e}_1) \right] \phi_{n'} \left(\mathbf{u} - \frac{w}{2} \mathbf{e}_3 \right) \phi_0 \left(\mathbf{u} + \frac{w}{2} \mathbf{e}_3 \right) \\ &\quad \times w^2 \sin \theta d^3 \mathbf{u} dw d\theta. \end{aligned} \quad (34)$$

Equation (34) contains a 5-dimensional integral over \mathbf{u} , w , and θ . In order to solve it efficiently we note that the integrand consists of two parts: one is the differential cross section $K_{F'F''} dP_{F|F'F''}/d\hat{\Omega}$, which does not depend on \mathbf{u} , n , or n' ; and the

other is the product of basis functions, which does not depend on F , F' , or F'' and can be evaluated independently of the atomic physics. Therefore we define the integral of three basis functions

$$C_{nn'}(w, \theta) = \int \phi_n \left[\mathbf{u} + \frac{w}{2}(\cos \theta \mathbf{e}_3 + \sin \theta \mathbf{e}_1) \right] \phi_{n'} \left(\mathbf{u} - \frac{w}{2} \mathbf{e}_3 \right) \phi_0 \left(\mathbf{u} + \frac{w}{2} \mathbf{e}_3 \right) d^3 \mathbf{u}. \quad (35)$$

It is readily seen that in our choice of basis, Eq. (19), the integrand takes on a special form. The basis function $\phi_n(\mathbf{v})$ is a Gaussian $e^{-v^2/2\sigma^2}$ times a polynomial of order $2n$ in the components (v_1, v_2, v_3) of \mathbf{v} . Therefore the integrand in Eq. (35) is equal to a polynomial of order $2(n+n')$ times the product of Gaussians

$$\begin{aligned} & \exp \left\{ -\frac{1}{2\sigma^2} \left[\mathbf{u} + \frac{w}{2}(\cos \theta \mathbf{e}_3 + \sin \theta \mathbf{e}_1) \right]^2 \right\} \exp \left[-\frac{1}{2\sigma^2} \left(\mathbf{u} - \frac{w}{2} \mathbf{e}_3 \right)^2 \right] \exp \left[-\frac{1}{2\sigma^2} \left(\mathbf{u} + \frac{w}{2} \mathbf{e}_3 \right)^2 \right] \\ & \propto \exp \left\{ -\frac{3}{2\sigma^2} \left[\mathbf{u} + \frac{w}{6}(\cos \theta \mathbf{e}_3 + \sin \theta \mathbf{e}_1) \right]^2 \right\}, \end{aligned} \quad (36)$$

where the proportionality constant is independent of \mathbf{u} . In 1 dimension the N -point Gauss-Hermite integration formula gives an exact result for products of polynomials of degree $< 2N$ and Gaussians. The same is true in 3 dimensions for the N^3 -point integration formula obtained by performing Gauss-Hermite integration on each of the three coordinate axes. In this case it is necessary to choose the weights corresponding to a centroid $w(\cos \theta \mathbf{e}_3 + \sin \theta \mathbf{e}_1)/6$ and 1σ width $\sigma/\sqrt{3}$, and take $N > n+n'$. The computational demand can be reduced by noting that the integrand in Eq. (35) is even under the substitution $u_2 \rightarrow -u_2$. Substituting in Eq. (35) we obtain

$$\mathcal{I} = 8\pi^2 \int \sum_{F''} y_{F''}(T_k) K_{F'F''}(w) \frac{dP_{F|F'F''}}{d\hat{\Omega}} C_{nn'}(w, \theta) w^2 \sin \theta dw d\theta. \quad (37)$$

As noted earlier, the remaining two integrals in Eq. (21) can be evaluated by replacing $dP_{F|F'F''}/d\hat{\Omega}$ with $\delta_{FF'}\delta^{(2)}(\hat{\Omega} + \hat{\mathbf{w}})$ and $\delta_{FF''}\delta^{(2)}(\hat{\Omega} - \hat{\mathbf{w}})$. This yields

$$\begin{aligned} X_{F_n, F' n'}^{(\text{col}, \text{H-H})} &= 8\pi^2 (4\pi\sigma^2)^{3/2} \int \sum_{F''} y_{F''}(T_k) K_{F'F''}(w) \left[\delta_{FF'}\delta^{(2)}(\hat{\Omega} + \hat{\mathbf{w}}) + \delta_{FF''}\delta^{(2)}(\hat{\Omega} - \hat{\mathbf{w}}) - \frac{dP_{F|F'F''}}{d\hat{\Omega}} \right] \\ &\quad \times C_{nn'}(w, \theta) w^2 \sin \theta dw d\theta. \end{aligned} \quad (38)$$

The δ functions of $\hat{\Omega}$ can be converted to functions of θ according to the standard prescription

$$2\pi\delta^{(2)}(\hat{\Omega} + \hat{\mathbf{w}}) \sin \theta = \delta(\theta - \pi) \quad \text{and} \quad 2\pi\delta^{(2)}(\hat{\Omega} - \hat{\mathbf{w}}) \sin \theta = \delta(\theta). \quad (39)$$

Thus

$$\begin{aligned} X_{F_n, F' n'}^{(\text{col}, \text{H-H})} &= 4\pi (4\pi\sigma^2)^{3/2} \left[\delta_{FF'} \int \sum_{F''} y_{F''}(T_k) K_{F'F''}(w) C_{nn'}(w, \pi) w^2 dw + \int y_F(T_k) K_{F'F}(w) C_{nn'}(w, 0) w^2 dw \right. \\ &\quad \left. - 2\pi \int \sum_{F''} y_{F''}(T_k) K_{F'F''}(w) \frac{dP_{F|F'F''}}{d\hat{\Omega}} C_{nn'}(w, \theta) w^2 \sin \theta dw d\theta \right]. \end{aligned} \quad (40)$$

Since we are only computing $X_{F_n, F' n'}^{(\text{col}, \text{H-H})}$ to zeroth order in T_* it is permissible to set $y_F(T_k) \rightarrow (2F+1)/4$. Making this substitution and recalling that $K_{F'F''}(w) = w\sigma_{F'F''}(w)$ we arrive at

$$\begin{aligned} X_{F_n, F' n'}^{(\text{col}, \text{H-H})} &= \pi (4\pi\sigma^2)^{3/2} \left[\delta_{FF'} \int \sum_{F''} (2F''+1) \sigma_{F'F''}(w) C_{nn'}(w, \pi) w^3 dw + \int (2F+1) \sigma_{F'F}(w) C_{nn'}(w, 0) w^3 dw \right. \\ &\quad \left. - 2\pi \int \sum_{F''} (2F''+1) \sigma_{F'F''}(w) \frac{dP_{F|F'F''}}{d\hat{\Omega}} C_{nn'}(w, \theta) w^3 \sin \theta dw d\theta \right]. \end{aligned} \quad (41)$$

5 INCLUSION OF HELIUM

In reality the primordial baryonic matter did not contain only ^1H but also ^4He with an abundance $n(^4\text{He})/n(^1\text{H}) \approx 0.08$ as well as trace quantities ($< 10^{-4}$) of ^2H , ^3He , and ^7Li . Collisions with the rare species will be unimportant compared to collisions with ^1H but for precision at the level of several percent it is worth considering the role of ^1H - ^4He collisions. Helium is an electron spin singlet and hence it cannot undergo spin exchange in collisions with hydrogen; thus in the usual approximation of a single spin temperature it does not do anything. If the spin-resolved velocity distribution is nonthermal however, collisions with helium can redistribute the velocities of the $F=0$ and $F=1$ hydrogen atoms and bring them closer to the Maxwellian distribution. Indeed if the $^4\text{He}/^1\text{H}$ ratio were very large, so that collisions with He atoms redistributed

the velocities faster than collisions with H atoms could change the hyperfine level populations, then one would expect the spin-resolved H velocity distribution to be Maxwellian and the single spin temperature approximation to become exact.

In this section we expand the Boltzmann equation to include the effects of helium. The first step is to introduce the Maxwellian distribution for helium and the appropriate basis modes for describing perturbations of the helium distribution function. We may then write the appropriate terms in the Boltzmann equation to account for H-He and He-He collisions.

In analogy with Eq. (19) we define helium basis modes

$$\phi_{\text{He},n}(\mathbf{v}) = 2^{-n-5/2} \pi^{-3/2} [(2n+1)!]^{-1/2} \frac{m_{\text{He}}}{k_B T_k v} H_{2n+1} \left(\frac{v}{\sqrt{k_B T_k / m_{\text{He}}}} \right) e^{-m_{\text{He}} v^2 / 2k_B T_k}, \quad (42)$$

which satisfy the orthonormality relation

$$\int \phi_{\text{He},n}^*(\mathbf{v}) \phi_{\text{He},n'}(\mathbf{v}) d^3 \mathbf{v} = \left(\frac{m_{\text{He}}}{4\pi k_B T_k} \right)^{3/2} \delta_{nn'}. \quad (43)$$

Note that the Maxwellian distribution is simply $\Phi_{\text{He}}(\mathbf{v}) = \phi_{\text{He},0}(\mathbf{v})$, and the thermal helium distribution function is $f_{\text{He}}^{(\text{th})}(\mathbf{v}) = n_{\text{HeI}} \Phi_{\text{He}}(\mathbf{v})$. We may then define the perturbation

$$\xi_{\text{He}}(\mathbf{v}) = f_{\text{He}}(\mathbf{v}) - f_{\text{He}}^{(\text{th})}(\mathbf{v}) = \sum_n \xi_{\text{He},n} \phi_{\text{He},n}(\mathbf{v}). \quad (44)$$

We now seek a linearized form of the Boltzmann equation for the H-He and He-He terms in analogy to Eq. (41). The spin exchange mechanism does not operate in H-He collisions since He is a spin singlet ($S = 0$). Therefore the H atom has the same value of F before and after the collision, and the H-He collision term in the Boltzmann equation for H is

$$f_F^{(\text{col,H-He})}(\mathbf{v}) = - \int K^{(\text{H-He})}(\mathbf{v}' - \mathbf{v}) f_F(\mathbf{v}) f_{\text{He}}(\mathbf{v}') d^3 \mathbf{v}' + \int K^{(\text{H-He})}(\mathbf{v}'' - \mathbf{v}') f_{\text{He}}(\mathbf{v}') f_F(\mathbf{v}'') p_{\text{H}}^{(\text{H-He})}(\mathbf{v}|\mathbf{v}', \mathbf{v}'') d^3 \mathbf{v}' d^3 \mathbf{v}''. \quad (45)$$

Here $K^{(\text{H-He})}(w)$ is the product of relative velocity and cross section at relative velocity w , and $p_{\text{H}}^{(\text{H-He})}(\mathbf{v}|\mathbf{v}', \mathbf{v}'')$ is the probability density for the final velocity of the H atom. Writing this in terms of perturbation variables gives

$$\begin{aligned} \dot{\xi}_F^{(\text{col,H-He})}(\mathbf{v}) &= - \int K^{(\text{H-He})}(\mathbf{v}' - \mathbf{v}) [\xi_F(\mathbf{v}) f_{\text{He}}^{(\text{th})}(\mathbf{v}') + f_F^{(\text{th})}(\mathbf{v}) \xi_{\text{He}}(\mathbf{v}')] d^3 \mathbf{v}' \\ &\quad + \int K^{(\text{H-He})}(\mathbf{v}'' - \mathbf{v}') [f_{\text{He}}^{(\text{th})}(\mathbf{v}') \xi_F(\mathbf{v}'') + \xi_{\text{He}}(\mathbf{v}') f_F^{(\text{th})}(\mathbf{v}'')] p_{\text{H}}^{(\text{H-He})}(\mathbf{v}|\mathbf{v}', \mathbf{v}'') d^3 \mathbf{v}' d^3 \mathbf{v}'', \end{aligned} \quad (46)$$

where we have used the fact that the zeroth-order terms on the right-hand side vanish. We have also dropped the second-order terms in ξ .

Integration of Eq. (46) against $\phi_n(\mathbf{v})$ gives

$$\dot{\xi}_{Fn}^{(\text{col,H-He})} = -n_{\text{HeI}} \sum_{n'} Y_{nn'} \xi_{Fn'}^{(\text{col,H-He})} - n_{\text{HI}} \sum_{n'} X_{Fn,\text{He } n'}^{(\text{col,H-He})} \xi_{\text{He},n'}^{(\text{col,H-He})}, \quad (47)$$

where the coefficients are:

$$\begin{aligned} Y_{nn'} &= (4\pi\sigma^2)^{3/2} \left[\int K^{(\text{H-He})}(\mathbf{v}' - \mathbf{v}) \phi_n(\mathbf{v}) \phi_{n'}(\mathbf{v}) \phi_{\text{He},0}(\mathbf{v}') d^3 \mathbf{v} d^3 \mathbf{v}' \right. \\ &\quad \left. - \int K^{(\text{H-He})}(\mathbf{v}'' - \mathbf{v}') \phi_n(\mathbf{v}) \phi_{\text{He},0}(\mathbf{v}') \phi_{n'}(\mathbf{v}'') p_{\text{H}}^{(\text{H-He})}(\mathbf{v}|\mathbf{v}', \mathbf{v}'') d^3 \mathbf{v} d^3 \mathbf{v}' d^3 \mathbf{v}'' \right] \end{aligned} \quad (48)$$

and

$$\begin{aligned} X_{Fn,\text{He } n'}^{(\text{col,H-He})} &= y_F(T_k) (4\pi\sigma^2)^{3/2} \left[\int K^{(\text{H-He})}(\mathbf{v}' - \mathbf{v}) \phi_n(\mathbf{v}) \phi_0(\mathbf{v}) \phi_{\text{He},n'}(\mathbf{v}') d^3 \mathbf{v} d^3 \mathbf{v}' \right. \\ &\quad \left. - \int K^{(\text{H-He})}(\mathbf{v}'' - \mathbf{v}') \phi_n(\mathbf{v}) \phi_{\text{He},n'}(\mathbf{v}') \phi_0(\mathbf{v}'') p_{\text{H}}^{(\text{H-He})}(\mathbf{v}|\mathbf{v}', \mathbf{v}'') d^3 \mathbf{v} d^3 \mathbf{v}' d^3 \mathbf{v}'' \right]. \end{aligned} \quad (49)$$

It will turn out that we need only explicitly evaluate $Y_{nn'}$ as $X_{Fn,\text{He } n'}^{(\text{col,H-He})}$ will not affect the hydrogen level populations at linear order in perturbation theory because, as we show below, in the steady state $\xi_{\text{He } n} = 0$.

As in our analysis of H-H collisions the most efficient way to evaluate $Y_{nn'}$ is to focus on the second integral in brackets in Eq. (48). Substitution of $p_{\text{H}}^{(\text{col,H-He})}(\mathbf{v}|\mathbf{v}', \mathbf{v}'') \rightarrow \delta^{(3)}(\mathbf{v} - \mathbf{v}'')$ recovers the first term. The evaluation of the integral is most easily accomplished by considering the centre-of-mass and relative velocities rather than \mathbf{v}' and \mathbf{v}'' as variables:

$$\mathbf{u} = \frac{m_{\text{H}} \mathbf{v}'' + m_{\text{He}} \mathbf{v}'}{m_{\text{H}} + m_{\text{He}}} \quad \text{and} \quad \mathbf{w} = \mathbf{v}'' - \mathbf{v}'; \quad d^3 \mathbf{v}' d^3 \mathbf{v}'' = d^3 \mathbf{u} d^3 \mathbf{w}. \quad (50)$$

The probability distribution for the final velocity \mathbf{v} in the scattering event is given by the analogue of Eq. (27)

$$p_{\text{H}}^{(\text{col,H-He})}(\mathbf{v}|\mathbf{v}', \mathbf{v}'') d^3\mathbf{v} = \frac{dP}{d\hat{\Omega}} d^2\hat{\Omega}, \quad (51)$$

and the specific relation between \mathbf{v} and $\hat{\Omega}$ is now

$$\mathbf{v} = \mathbf{u} + \frac{m_{\text{He}}}{m_{\text{H}} + m_{\text{He}}} \mathbf{w}, \quad (52)$$

which is different from Eq. (28) since the He and H masses are unequal. The second integral in Eq. (48) then becomes

$$\begin{aligned} \mathcal{I}_2 &\equiv \int K^{(\text{H-He})}(\mathbf{v}'' - \mathbf{v}') \phi_n(\mathbf{v}) \phi_{\text{He},0}(\mathbf{v}') \phi_{n'}(\mathbf{v}'') p_{\text{H}}^{(\text{H-He})}(\mathbf{v}|\mathbf{v}', \mathbf{v}'') d^3\mathbf{v} d^3\mathbf{v}' d^3\mathbf{v}'' \\ &= \int K^{(\text{H-He})}(w) \phi_n \left(\mathbf{u} + \frac{m_{\text{He}}}{m_{\text{H}} + m_{\text{He}}} \hat{\Omega} \right) \phi_{\text{He},0} \left(\mathbf{u} - \frac{m_{\text{H}}}{m_{\text{H}} + m_{\text{He}}} \mathbf{w} \right) \phi_{n'} \left(\mathbf{u} + \frac{m_{\text{He}}}{m_{\text{H}} + m_{\text{He}}} \mathbf{w} \right) \frac{dP}{d\hat{\Omega}} d^3\mathbf{u} d^3\mathbf{w} d^2\hat{\Omega} \\ &= 4\pi \int K^{(\text{H-He})}(w) \phi_n \left(\mathbf{u} + \frac{m_{\text{He}} w \hat{\Omega}}{m_{\text{H}} + m_{\text{He}}} \right) \phi_{\text{He},0} \left(\mathbf{u} - \frac{m_{\text{H}} w \mathbf{e}_3}{m_{\text{H}} + m_{\text{He}}} \right) \phi_{n'} \left(\mathbf{u} + \frac{m_{\text{He}} w \mathbf{e}_3}{m_{\text{H}} + m_{\text{He}}} \right) \frac{dP}{d\hat{\Omega}} w^2 d^3\mathbf{u} dw d^2\hat{\Omega}. \end{aligned} \quad (53)$$

In the last line we have used spherical symmetry to choose \mathbf{w} to be in the third coordinate direction and replace $d^3\mathbf{w}$ with $4\pi w^2 dw$. If we write $\hat{\Omega}$ in spherical coordinates (Eq. 33) and integrate out the φ direction we then get

$$\begin{aligned} \mathcal{I}_2 &= 8\pi^2 \int K^{(\text{H-He})}(w) \phi_n \left[\mathbf{u} + \frac{m_{\text{He}} w (\cos\theta \mathbf{e}_3 + \sin\theta \mathbf{e}_1)}{m_{\text{H}} + m_{\text{He}}} \right] \phi_{\text{He},0} \left(\mathbf{u} - \frac{m_{\text{H}} w \mathbf{e}_3}{m_{\text{H}} + m_{\text{He}}} \right) \phi_{n'} \left(\mathbf{u} + \frac{m_{\text{He}} w \mathbf{e}_3}{m_{\text{H}} + m_{\text{He}}} \right) \\ &\quad \times \frac{dP}{d\hat{\Omega}} w^2 \sin\theta d^3\mathbf{u} dw d\theta. \end{aligned} \quad (54)$$

Once again it is possible to separate the purely kinematic terms in this integral from the cross sections. We define

$$D_{nn'}(w, \theta) = \int \phi_n \left[\mathbf{u} + \frac{m_{\text{He}} w (\cos\theta \mathbf{e}_3 + \sin\theta \mathbf{e}_1)}{m_{\text{H}} + m_{\text{He}}} \right] \phi_{\text{He},0} \left(\mathbf{u} - \frac{m_{\text{H}} w \mathbf{e}_3}{m_{\text{H}} + m_{\text{He}}} \right) \phi_{n'} \left(\mathbf{u} + \frac{m_{\text{He}} w \mathbf{e}_3}{m_{\text{H}} + m_{\text{He}}} \right) d^3\mathbf{u}, \quad (55)$$

so that

$$\mathcal{I}_2 = 8\pi^2 \int K^{(\text{H-He})}(w) \frac{dP}{d\hat{\Omega}} D_{nn'}(w, \theta) w^2 \sin\theta dw d\theta. \quad (56)$$

Just as for $C_{nn'}$, it is possible to evaluate $D_{nn'}$ exactly by Gauss-Hermite integration on each of the three coordinate axes. However in this case the centroid of integration is at $-m_{\text{H}} m_{\text{He}} w (\cos\theta \mathbf{e}_3 + \sin\theta \mathbf{e}_1) / [(m_{\text{H}} + m_{\text{He}})(2m_{\text{H}} + m_{\text{He}})]$ and the 1σ width is $\sqrt{k_B T_k / (2m_{\text{H}} + m_{\text{He}})}$.

With this value for \mathcal{I}_2 , and recalling that the first integral in Eq. (48) can be obtained from the second by the replacement $p_{\text{H}}^{(\text{col,H-He})}(\mathbf{v}|\mathbf{v}', \mathbf{v}'') \rightarrow \delta^{(3)}(\mathbf{v} - \mathbf{v}'')$, or equivalently $dP/d\hat{\Omega} \rightarrow \delta^{(2)}(\hat{\Omega} - \hat{\mathbf{w}})$, we find

$$\begin{aligned} Y_{nn'} &= (4\pi\sigma^2)^{3/2} \left[8\pi^2 \int K^{(\text{H-He})}(w) \delta^{(2)}(\hat{\Omega} - \hat{\mathbf{w}}) D_{nn'}(w, \theta) w^2 \sin\theta dw d\theta \right. \\ &\quad \left. - 8\pi^2 \int K^{(\text{H-He})}(w) \frac{dP}{d\hat{\Omega}} D_{nn'}(w, \theta) w^2 \sin\theta dw d\theta \right]. \end{aligned} \quad (57)$$

Using Eq. (39) this simplifies further to

$$Y_{nn'} = (4\pi\sigma^2)^{3/2} \left[\int K^{(\text{H-He})}(w) D_{nn'}(w, 0) w^2 dw - 2\pi \int K^{(\text{H-He})}(w) \frac{dP}{d\hat{\Omega}} D_{nn'}(w, \theta) w^2 \sin\theta dw d\theta \right], \quad (58)$$

which is now suitable for numerical evaluation.

6 SOLUTION OF THE BOLTZMANN EQUATION

We are now interested in the steady-state solution to Eq. (7). For simplicity we restrict our attention to the case of a purely atomic gas of H and He and no Ly α radiation. These conditions are expected to pertain to the era before the first sources of ultraviolet and X-ray radiation.

6.1 The solution

As currently constructed the Boltzmann equation can be written as

$$\dot{\xi} = -\mathbf{X}\xi + \mathbf{S}, \quad (59)$$

where \mathbf{X} is the relaxation matrix and \mathbf{S} is the forcing term. The dimension of the vectors $\boldsymbol{\xi}$ and \mathbf{S} is $3N$, where N is the number of basis modes used. There are N modes each for the perturbations in the hydrogen $F = 0$ phase space density, for hydrogen $F = 1$, and for helium. The forcing term is purely radiative

$$S_{1n} = -S_{0n} = \frac{3}{4}A \left(\frac{T_\gamma}{T_k} - 1 \right) n_{\text{HI}} \delta_{n,0}, \quad (60)$$

and can be read off from Eq. (20) along with $S_{\text{He},n} = 0$. The relaxation matrix is

$$\mathbf{X} = \mathbf{X}^{(\text{rad})} + n_{\text{HI}} \mathbf{X}^{(\text{col,H-H})} + n_{\text{HI}} \mathbf{X}^{(\text{col,H-He})} + n_{\text{HI}} \mathbf{X}^{(\text{col,He-He})}. \quad (61)$$

The various contributions to the relaxation matrix exhibit sparseness patterns when broken into the blocks corresponding to H($F = 0$), H($F = 1$), and He. This turns out to be very useful in solving the Boltzmann equation because only some of the rates are relevant. The radiative contribution can be read off from Eq. (20) and it breaks down as

$$\mathbf{X}^{(\text{rad})} = \frac{T_\gamma}{T_\star} A \begin{pmatrix} \mathbf{I} & -3\mathbf{I} & 0 \\ -\mathbf{I} & 3\mathbf{I} & 0 \\ 0 & 0 & 0 \end{pmatrix}, \quad (62)$$

where \mathbf{I} is the $N \times N$ identity matrix. The H-H collision term only has non-zero entries for the hydrogen atoms,

$$\mathbf{X}^{(\text{col,H-H})} = \begin{pmatrix} \mathbf{X}_{00}^{(\text{col,H-H})} & \mathbf{X}_{01}^{(\text{col,H-H})} & 0 \\ \mathbf{X}_{10}^{(\text{col,H-H})} & \mathbf{X}_{11}^{(\text{col,H-H})} & 0 \\ 0 & 0 & 0 \end{pmatrix}. \quad (63)$$

The H-He collision term has a particular structure due to the elastic cross section being the same for H($F = 0$) and H($F = 1$), and because the spin-exchange cross section vanishes:

$$\mathbf{X}^{(\text{col,H-He})} = \begin{pmatrix} (n_{\text{HeI}}/n_{\text{HI}})\mathbf{Y} & 0 & \mathbf{X}_{0\text{He}}^{(\text{col,H-He})} \\ 0 & (n_{\text{HeI}}/n_{\text{HI}})\mathbf{Y} & \mathbf{X}_{1\text{He}}^{(\text{col,H-He})} \\ \mathbf{X}_{\text{He0}}^{(\text{col,H-He})} & \mathbf{X}_{\text{He1}}^{(\text{col,H-He})} & \mathbf{X}_{\text{HeHe}}^{(\text{col,H-He})} \end{pmatrix}, \quad (64)$$

where $\mathbf{X}_{\text{He0}}^{(\text{col,H-He})} = \mathbf{X}_{\text{He1}}^{(\text{col,H-He})}$, and \mathbf{Y} is the matrix of H-He collision integrals defined in Eq. (48).

Finally, for the He-He term, only the $\mathbf{X}_{\text{HeHe}}^{(\text{col,He-He})}$ block is nonzero.

The key to solving the Boltzmann equation is to introduce the change of basis from the abundances of H($F = 0$) and H($F = 1$) to the new modes

$$\xi'_{\Delta,n} = \xi_{1,n} - 3\xi_{0,n}, \quad \xi'_{\Sigma,n} = \xi_{1,n} + \xi_{0,n}, \quad \text{and} \quad \xi'_{\text{He},n} = \xi_{\text{He},n}. \quad (65)$$

The new basis $\{\xi'_{\Delta,n}, \xi'_{\Sigma,n}, \xi'_{\text{He},n}\}$ is related to the old basis $\{\xi_{0,n}, \xi_{1,n}, \xi_{\text{He},n}\}$ by a matrix,

$$\boldsymbol{\xi}' = \mathbf{R}\boldsymbol{\xi}, \quad \mathbf{R} = \begin{pmatrix} -3\mathbf{I} & \mathbf{I} & 0 \\ \mathbf{I} & \mathbf{I} & 0 \\ 0 & 0 & \mathbf{I} \end{pmatrix}. \quad (66)$$

The relaxation matrices \mathbf{X} can be expressed in the new basis via $\mathbf{X}' = \mathbf{R}\mathbf{X}\mathbf{R}^{-1}$, and the source is expressed as $\mathbf{S}' = \mathbf{R}\mathbf{S}$. It is at this point that a simplification occurs. Although \mathbf{X} is in general non-sparse (cf. Eqs. 62–64), the first column of blocks of \mathbf{X}' read as follows:

$$\begin{aligned} \mathbf{X}'_{\Delta\Delta} &= 4\frac{T_\gamma}{T_\star} A\mathbf{I} + \frac{n_{\text{HI}}}{4} [3\mathbf{X}_{00}^{(\text{col,H-H})} - 3\mathbf{X}_{01}^{(\text{col,H-H})} - \mathbf{X}_{10}^{(\text{col,H-H})} + \mathbf{X}_{11}^{(\text{col,H-H})}] + n_{\text{HeI}}\mathbf{Y}, \\ \mathbf{X}'_{\Sigma\Delta} &= \frac{n_{\text{HI}}}{4} [-\mathbf{X}_{00}^{(\text{col,H-H})} + \mathbf{X}_{01}^{(\text{col,H-H})} - \mathbf{X}_{10}^{(\text{col,H-H})} + \mathbf{X}_{11}^{(\text{col,H-H})}] = \frac{n_{\text{HI}}}{2} \sum_{F,F'} (-1)^{F'-1} \mathbf{X}_{FF'}^{(\text{col,H-H})}, \quad \text{and} \\ \mathbf{X}'_{\text{He}\Delta} &= 0. \end{aligned} \quad (67)$$

The latter expression may be evaluated by substituting Eq. (41) in for $X_{FF'}^{(\text{col,H-H})}$. This gives

$$\begin{aligned} X'_{\Sigma n, \Delta n'} &= \pi(4\pi\sigma^2)^{3/2} \frac{n_{\text{HI}}}{4} \left[\int \sum_{F,F'} (-1)^{F'-1} (2F+1) \sigma_{F'F}(w) C_{nn'}(w, 0) w^3 dw \right. \\ &\quad \left. - 2\pi \int \sum_{F,F',F''} (-1)^{F'-1} (2F''+1) \sigma_{F'F''}(w) \frac{dP_{F|F'F''}}{d\hat{\Omega}} C_{nn'}(w, \theta) w^3 \sin\theta dw d\theta \right]. \end{aligned} \quad (68)$$

(The first term in the square brackets in Eq. 41 does not contribute because it trivially cancels when summed over F' .) Using Eq. (B8), one may verify directly that

$$\sum_{F, F', F''} (-1)^{F'-1} (2F'' + 1) \sigma_{F'F''}(w) \frac{dP_{F|F'F''}}{d\hat{\Omega}} = 0 \quad (69)$$

for all w and θ and hence the last integral in Eq. (68) vanishes. By integrating Eq. (69) over angles, we find

$$2 \sum_{F, F''} (-1)^{F'-1} (2F'' + 1) \sigma_{F'F''}(w) = \int \sum_{F, F', F''} (-1)^{F'-1} (2F'' + 1) \sigma_{F'F''}(w) \frac{dP_{F|F'F''}}{d\hat{\Omega}} d\hat{\Omega} = 0. \quad (70)$$

Noting that the total cross section is symmetrical, $\sigma_{F'F''}(w) = \sigma_{F''F'}(w)$, and that F'' is a dummy variable in the summation in Eq. (70), we see that in fact the first integral in Eq. (68) also vanishes, so that $X'_{\Sigma n, \Delta n'} = 0$. Therefore the matrix \mathbf{X}' , and in particular its first column, reads

$$\mathbf{X}' = \begin{pmatrix} \mathbf{X}'_{\Delta\Delta} & \mathbf{X}'_{\Delta\Sigma} & \mathbf{X}'_{\Delta\text{He}} \\ 0 & \mathbf{X}'_{\Sigma\Sigma} & \mathbf{X}'_{\Sigma\text{He}} \\ 0 & \mathbf{X}'_{\text{He}\Sigma} & \mathbf{X}'_{\text{HeHe}} \end{pmatrix}. \quad (71)$$

As we are about to see, we will only need to evaluate the first column of \mathbf{X}' . The source vector in the new basis is

$$S'_{\Delta, n} = 3A \left(\frac{T_\gamma}{T_k} - 1 \right) n_{\text{HI}} \delta_{n, 0}, \quad S'_{\Sigma, n} = 0, \quad S'_{\text{He}, n} = 0. \quad (72)$$

Thus only one entry of the vector \mathbf{S}' is nonzero.

The particular sparseness patterns of \mathbf{X}' and \mathbf{S}' are useful because they imply that the evolution of $\xi'_{\Sigma, n}$ and $\xi'_{\text{He}, n}$ does not depend on $\xi'_{\Delta, n}$ and has no sources. Therefore these components of ξ' – and more generally, the corresponding distribution functions $f_0(\mathbf{v}) + f_1(\mathbf{v})$ and $f_{\text{He}}(\mathbf{v})$ – will relax to thermal equilibrium. We have chosen to expand our distribution functions around the thermal equilibrium solution at temperature T_k and hence we will have

$$\xi'_{\Sigma, n} = \xi'_{\text{He}, n} = 0. \quad (73)$$

This result allows us to simplify the equation for $\xi'_{\Delta, n}$ to yield $\dot{\xi}'_{\Delta, n} = -\sum_{n'} X'_{\Delta n, \Delta n'} \xi'_{\Delta, n'} + S'_{\Delta, n}$. If we consider the steady-state solution with $\dot{\xi}'_{\Delta, n} = 0$ we conclude that

$$\xi'_{\Delta} = (\mathbf{X}'_{\Delta\Delta})^{-1} \mathbf{S}'_{\Delta}. \quad (74)$$

Numerical evaluation of Eq. (74) can be simplified by exploiting the result $\mathbf{X}'_{\Sigma\Delta} = 0$ and using Eq. (67) to write

$$\mathbf{X}'_{\Delta\Delta} = \mathbf{X}'_{\Delta\Delta} - \mathbf{X}'_{\Sigma\Delta} = 4 \frac{T_\gamma}{T_*} \mathbf{A} \mathbf{I} + n_{\text{HI}} [\mathbf{X}'_{00}^{(\text{col}, \text{H-H})} - \mathbf{X}'_{01}^{(\text{col}, \text{H-H})}] + n_{\text{HeI}} \mathbf{Y}, \quad (75)$$

so that

$$\xi'_{\Delta, n} = 3A \left(\frac{T_\gamma}{T_k} - 1 \right) n_{\text{HI}} \left(\left\{ 4 \frac{T_\gamma}{T_*} \mathbf{A} \mathbf{I} + n_{\text{HI}} [\mathbf{X}'_{00}^{(\text{col}, \text{H-H})} - \mathbf{X}'_{01}^{(\text{col}, \text{H-H})}] + n_{\text{HeI}} \mathbf{Y} \right\}_{n0}^{-1} \right), \quad (76)$$

where the subscript $()_{n0}$ denotes the entry in the row corresponding to the n th basis mode and the column corresponding to the 0th mode.

6.2 A subtlety: CMB heating of the gas

Before continuing, we discuss one subtlety of the steady-state solution to the Boltzmann equation, Eq. (76). The method of solution depends on the observation that $\mathbf{X}'_{\Sigma\Delta} = 0$, which we proved for the elastic approximation cross sections. It is natural to ask whether $\mathbf{X}'_{\Sigma\Delta} = 0$ would still be true if we dropped the elastic approximation and used the full cross sections instead. While the answer to this questions is in fact no, and this drastically alters the steady-state solution to Eq. (59) if the full (inelastic) cross sections are used, the solution of Eq. (76) remains the physical solution to Eq. (7).

In addition to being an approximation for the cross sections, the elastic approximation (in the simple form used here) treats the scattering as elastic, i.e. the total kinetic energy of the atoms is the same before and after collision. For this reason, the elastic approximation does not include heating of the gas by the CMB in the 21-cm line (the process in which the CMB heats the spins, which then collisionally transfer energy to the kinetic degrees of freedom of the gas). Of course, if this process is taken into account, the only possible steady-state solution to Eq. (59) is for both the spin and kinetic degrees of freedom to come to thermal equilibrium with the CMB. Recall, however, that in the above derivation we dropped the explicitly time-dependent terms associated with the Hubble expansion because the Hubble time during this epoch is much longer than the radiative or collision times. As we show below, the 21-cm heating time is even *longer* than the Hubble time and thus, while in a nonexpanding universe the spin and kinetic degrees of freedom would have enough time to thermalize with the CMB, in our expanding Universe such heating is extremely inefficient. For this reason the solution to the Boltzmann equations derived in the previous section by neglecting processes with timescales longer than the Hubble time is the physical solution.

A relatively simple argument can be used to estimate the timescale for heating in the 21-cm line. In the spin temperature approximation, we know that the net rate of collisional de-excitation per H atom is

$$\Gamma_{\text{de-ex}} = n_{\text{HI}}[\langle\sigma_{10}v\rangle(T_k)y_0(T_s) - \langle\sigma_{01}v\rangle(T_k)y_1(T_s)] \approx \frac{3}{4}n_{\text{HI}}\langle\sigma_{10}v\rangle(T_k)T_*^2(T_k^{-1} - T_s^{-1}), \quad (77)$$

where $\langle\sigma_{10}v\rangle(T_k)$ is the thermally averaged cross section for de-excitation, and the approximation makes use of Eq. (3) and the principle of detailed balance $\langle\sigma_{01}v\rangle(T_k) = 3e^{-T_*/T_k}\langle\sigma_{10}v\rangle(T_k)$. The heating rate in the 21-cm line is then $k_B T_* \Gamma_{\text{de-ex}}$ per atom. Comparing this to the heat capacity for a monatomic gas, $C_v = 3k_B(1 + f_{\text{He}})/2$ per H atom, implies that the heating rate is

$$\dot{T}_k|_{21\text{ cm}} = \frac{k_B T_* \Gamma_{\text{de-ex}}}{C_v} = \frac{n_{\text{HI}}\langle\sigma_{10}v\rangle(T_k) T_*^2(T_k^{-1} - T_s^{-1})}{2(1 + f_{\text{He}})}, \quad (78)$$

implying a timescale for heating of the gas

$$t_h \equiv \frac{T_k}{\dot{T}_k|_{21\text{ cm}}} = \frac{2(1 + f_{\text{He}})T_k}{n_{\text{HI}}\langle\sigma_{10}v\rangle(T_k) T_*^2(T_k^{-1} - T_s^{-1})}. \quad (79)$$

Direct computation with the standard evolution of T_s shows that this is always much longer than the Hubble time, e.g. $t_h = 50$ Gyr versus $H^{-1} = 100$ Myr at $1 + z = 40$, and $t_h = 170$ Gyr versus $H^{-1} = 200$ Myr at $1 + z = 25$. A more refined analysis is possible using kinetic theory but since the heating timescale is so much longer than any other timescale in the problem we need not do this calculation.

7 LINE EMISSIVITY AND PROFILE

7.1 Determination of emissivity

Having determined the full distribution function for the various levels of hydrogen, we now turn to the problem of determining the 21 centimetre emissivity. This emissivity is most conveniently expressed using the time derivative of the photon phase space density \mathcal{N} . The phase space density is related to the familiar specific intensity via $\mathcal{N} = c^2 I_\nu / (2h\nu^3)$ and is more convenient for cosmological calculations because, unlike I_ν , it is conserved along a trajectory. Its time derivative is

$$\dot{\mathcal{N}} = \frac{c^3 \rho}{2h\nu^3} (j_\nu - \kappa_\nu I_\nu). \quad (80)$$

In this equation j_ν comes from spontaneous emission, whereas κ_ν comes from a combination of absorption and stimulated emission (the latter giving a negative contribution). The spontaneous emission term is given by the usual expression

$$j_\nu \rho = \frac{h\nu A}{4\pi} \left[\frac{dn_{\text{HI}}(F=1)}{dv_{\parallel} dV} \right] \left(\frac{dv_{\parallel}}{d\nu} \right) = \frac{hcA}{4\pi} \int f_1(\mathbf{v}) d^2\mathbf{v}_{\perp}, \quad (81)$$

where the component of velocity along the line of sight is $v_{\parallel} = c(1 - \nu/\nu_{10})$, \mathcal{V} is the volume, we have integrated over the irrelevant transverse velocity and assumed $|1 - \nu/\nu_{10}| \ll 1$. Since we have calculated the distribution function in the bulk rest frame of the gas v_{\parallel} is measured in this frame. The stimulated emission contribution is obtained by multiplying this by the photon phase space density \mathcal{N} and the absorption term is then obtained by replacing $f_1 \rightarrow f_0$ and multiplying by 3 to account for the lower statistical weight of the $F=0$ level:

$$-\kappa_\nu \rho I_\nu = \frac{hcA}{4\pi} \mathcal{N} \int [f_1(\mathbf{v}) - 3f_0(\mathbf{v})] d^2\mathbf{v}_{\perp}. \quad (82)$$

We thus find

$$\dot{\mathcal{N}} = \frac{c^4 A}{8\pi\nu^3} \left\{ \int f_1(\mathbf{v}) d^2\mathbf{v}_{\perp} + \mathcal{N} \int [f_1(\mathbf{v}) - 3f_0(\mathbf{v})] d^2\mathbf{v}_{\perp} \right\}. \quad (83)$$

Splitting $f_F(\mathbf{v})$ into the thermal piece $f_F^{(\text{th})}(\mathbf{v})$ and non-thermal piece $\xi_F(\mathbf{v})$ yields

$$\dot{\mathcal{N}} = \frac{c^4 A}{8\pi\nu^3} \left\{ [y_1(T_k) + \mathcal{N}y_1(T_k) - 3\mathcal{N}y_0(T_k)] n_{\text{HI}} \int \Phi_{T_k}(\mathbf{v}) d^2\mathbf{v}_{\perp} + \int \xi_1(\mathbf{v}) d^2\mathbf{v}_{\perp} + \mathcal{N} \int [\xi_1(\mathbf{v}) - 3\xi_0(\mathbf{v})] d^2\mathbf{v}_{\perp} \right\}. \quad (84)$$

In the limit where $T_* \ll T_k, T_\gamma$ we have

$$y_1(T_k) + \mathcal{N}y_1(T_k) - 3\mathcal{N}y_0(T_k) = \frac{e^{T_*/T_\gamma} (3e^{-T_*/T_k}) - 3}{(1 + 3e^{-T_*/T_k})(e^{T_*/T_\gamma} - 1)} \approx \frac{3}{4} \left(1 - \frac{T_\gamma}{T_k} \right). \quad (85)$$

Substituting this into Eq. (84) and re-expressing it in terms of basis modes we find

$$\dot{\mathcal{N}} = \frac{c^4 A}{8\pi\nu^3} \left[\frac{3}{4} \left(1 - \frac{T_\gamma}{T_k} \right) n_{\text{HI}} \psi_0(v_{\parallel}) + \sum_n \xi_{1n} \psi_n(v_{\parallel}) + \mathcal{N} \sum_n (\xi_{1n} - 3\xi_{0n}) \psi_n(v_{\parallel}) \right], \quad (86)$$

where $\psi_n(v_{\parallel}) = \int \phi_n(\mathbf{v}) d^2v_{\perp}$ is given by the formulas in Appendix A. Since $\xi'_{\Sigma,n} = 0$, we have $\xi_{1n} = \xi'_{\Delta,n}/4$ and since $\mathcal{N} \approx T_{\gamma}/T_{\star} \gg 1$ the third term dominates over the second. Thus we arrive at

$$\dot{\mathcal{N}} \approx \frac{c^4 A}{8\pi\nu_{10}^3} \left[\frac{3}{4} \left(1 - \frac{T_{\gamma}}{T_k} \right) n_{\text{HI}} \psi_0(v_{\parallel}) + \frac{T_{\gamma}}{T_{\star}} \sum_n \xi'_{\Delta,n} \psi_n(v_{\parallel}) \right]. \quad (87)$$

The observed brightness temperature T_b due to the H I 21-cm signal is obtained by the usual equation, $T_b = h\nu_{\text{obs}}\Delta\mathcal{N}/k_B$, where $\nu_{\text{obs}} = \nu_{10}/(1+z)$ is the observed frequency today and $\Delta\mathcal{N}$ is the change in the phase space density. This gives

$$T_b = \frac{h\nu_{10}}{k_B(1+z)} \Delta\mathcal{N} = \frac{T_{\star}}{1+z} \int \dot{\mathcal{N}} dt = \frac{T_{\star}}{c(1+z)} \int \dot{\mathcal{N}} \frac{dr_{\parallel}}{1+z} = \frac{T_{\star}}{c(1+z)^2} \int \dot{\mathcal{N}} dr_{\parallel}, \quad (88)$$

where r_{\parallel} is the comoving distance in the radial direction. In this equation $\dot{\mathcal{N}}$ should be evaluated using Eq. (87). Note that Eq. (87) depends on v_{\parallel} , which we have defined to be the radial velocity of the H atoms that contribute to the signal, relative to the bulk flow of the gas. This velocity is

$$v_{\parallel} \approx -\frac{H(z)}{1+z} [r_{\parallel} - R_{\parallel}(z)] - v_{\parallel}^{(\text{pec})}, \quad (89)$$

where $R_{\parallel}(z)$ is the radial comoving distance to redshift z in an unperturbed universe, $H(z)/(1+z)$ is the cosmological velocity gradient, and the peculiar velocity $v_{\parallel}^{(\text{pec})}$ is needed since the atom's velocity is measured relative to the gas and not to the Eulerian coordinate system. The negative sign is required since v_{\parallel} is the velocity of the atom relative to the gas (not the other way around) although in practice it does not matter since $\psi_n(v_{\parallel})$ is even.

7.2 Large-scale perturbations

For large-scale perturbations where the velocity gradient and density do not vary significantly across the line profile, Eqs. (88) and (89) can be combined to give

$$T_b = \left[\frac{H(z)}{1+z} + \frac{dv_{\parallel}^{(\text{pec})}}{dr_{\parallel}} \right]^{-1} \frac{T_{\star}}{c(1+z)^2} \int \dot{\mathcal{N}} dv_{\parallel}. \quad (90)$$

If we further use Eq. (87) for the line profile, we find

$$T_b = \left[\frac{H(z)}{1+z} + \frac{dv_{\parallel}^{(\text{pec})}}{dr_{\parallel}} \right]^{-1} \frac{3c^3 AT_{\star}}{32\pi\nu_{10}^3(1+z)^2} n_{\text{HI}} \left(1 - \frac{T_{\gamma}}{T_s^{\text{eff}}} \right), \quad (91)$$

where the effective spin temperature T_s^{eff} is given by

$$\frac{1}{T_s^{\text{eff}}} = \frac{1}{T_k} \int_{-\infty}^{\infty} \psi_0(v_{\parallel}) dv_{\parallel} - \frac{4}{3T_{\star}} \sum_n \frac{\xi'_{\Delta,n}}{n_{\text{HI}}} \int_{-\infty}^{\infty} \psi_n(v_{\parallel}) dv_{\parallel} = \frac{1}{T_k} - \frac{4}{3T_{\star}} \sum_n \frac{\sqrt{(2n+1)!} \xi'_{\Delta,n}}{2^n n! n_{\text{HI}}}. \quad (92)$$

This result should be compared with Eq. (4). Note that for the standard assumption of individual Maxwellian distributions for $F=0$ and $F=1$ (Eq. 24), we have $\xi'_{\Delta,n}|_{T_s} = -3T_{\star}(T_s^{-1} - T_k^{-1})n_{\text{HI}}\delta_{n,0}/4$, and hence $T_s^{\text{eff}}|_{T_s} = T_s$.

For linear-regime perturbations, one may write Eq. (91) as a function $T_b(z, \delta_b, dv_{\parallel}^{(\text{pec})}/dr_{\parallel})$. (We consider T_k , T_s^{eff} , and n_{HI} to be functions of δ_b .) We expand this as

$$T_b = \bar{T}_b \left(1 - \frac{1+z}{H(z)} \frac{dv_{\parallel}^{(\text{pec})}}{dr_{\parallel}} \right) + \frac{\partial T_b}{\partial \delta_b} \delta_b, \quad (93)$$

where \bar{T}_b is the brightness temperature at mean density with no peculiar velocity. Taking the power spectrum of Eq. (91), one may obtain (Barkana & Loeb 2005)

$$P_{T_b}(k) = P_{\mu^0}(k) + \mu^2 P_{\mu^2}(k) + \mu^4 P_{\mu^4}(k) \quad (94)$$

where $\mu = k_{\parallel}/k$ is the cosine of the angle between the line of sight and the wave vector,

$$P_{\mu^0}(k) = \left(\frac{\partial T_b}{\partial \delta_b} \right)^2 P_{\delta_b}(k), \quad P_{\mu^2}(k) = k \bar{T}_b \frac{\partial T_b}{\partial \delta_b} P_{\delta_b, v_b}(k), \quad \text{and} \quad P_{\mu^4}(k) = k^2 (\bar{T}_b)^2 P_{v_b}(k). \quad (95)$$

Here $P_{\delta_b}(k)$ is the power spectrum of the baryon density fluctuations, $P_{v_b}(k)$ is the power spectrum of the baryon velocity perturbations, and $P_{\delta_b, v_b}(k)$ is their cross-spectrum.⁵

⁵ Bharadwaj & Ali (2004) and Barkana & Loeb (2005) used the additional relation $v_b = \delta_b/k$, which is valid for linear evolution on large scales in the matter-dominated era.

Spin temperature at mean density

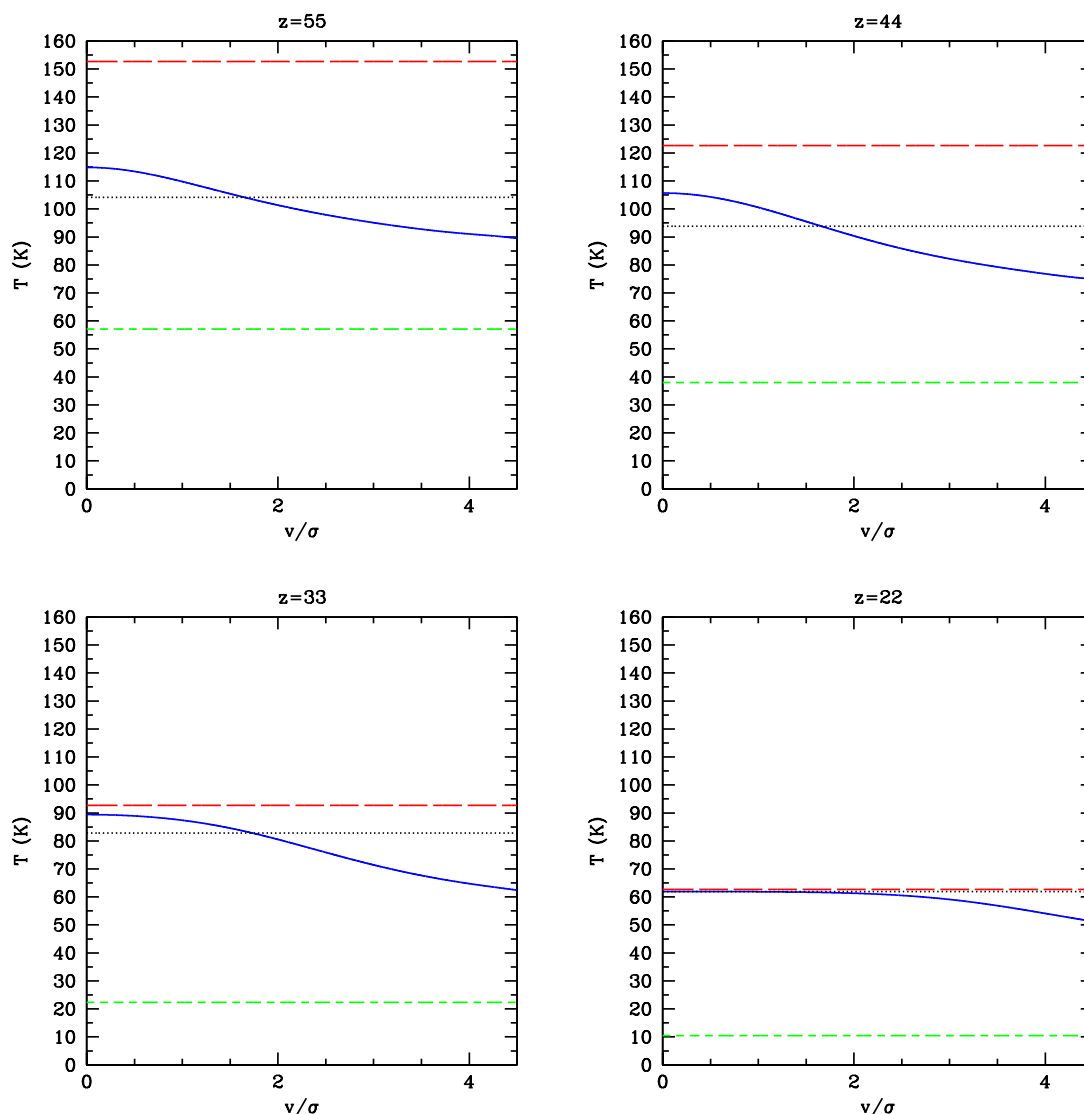


Figure 1. The temperature shown for mean density intergalactic gas at several redshifts. The solid (blue) curve is the spin temperature as a function of atomic velocity v ; the long-dashed (red) line is the CMB temperature; the short-dashed (green) line is the kinetic temperature; and the dotted (black) line is the spin temperature computed by the standard formula (Eq. 23 of Madau et al. 1997 with $y_\alpha = 0$). Note that the spin temperature is closer to the kinetic temperature for the fastest-moving atoms.

7.3 Results for high redshift intergalactic gas

We have computed the 21-cm emissivity and line profile for the high-redshift intergalactic gas. The CMB temperature was determined using the usual redshift scaling, $T_\gamma = (1+z)T_0$, where $T_0 = 2.728$ K is the present day temperature (Fixsen et al. 1996). The gas kinetic temperature was determined using RECFAST (Seager et al. 1999); we consider only the era before X-ray and shock heating become important in controlling the temperature of the gas. We do not know precisely when this occurred, but simulations show that even in the absence of astrophysical radiation sources, shocked minihaloes dominate the *mean* 21-cm signal at $z < 20$ (Shapiro et al. 2005), and probably dominate the power spectrum even sooner. We therefore cut off our plots at $z = 20$ but one should be aware that the approximation of adiabatically expanding unshocked gas may break down before then.

In Fig. 1, we show the spin temperature of the gas at mean density, as a function of the atom’s velocity. For the purposes of this figure, we defined a velocity-dependent spin temperature,

$$T_s(v) \equiv \frac{T_\star}{\ln[3f_0(v)/f_1(v)]}, \quad (96)$$

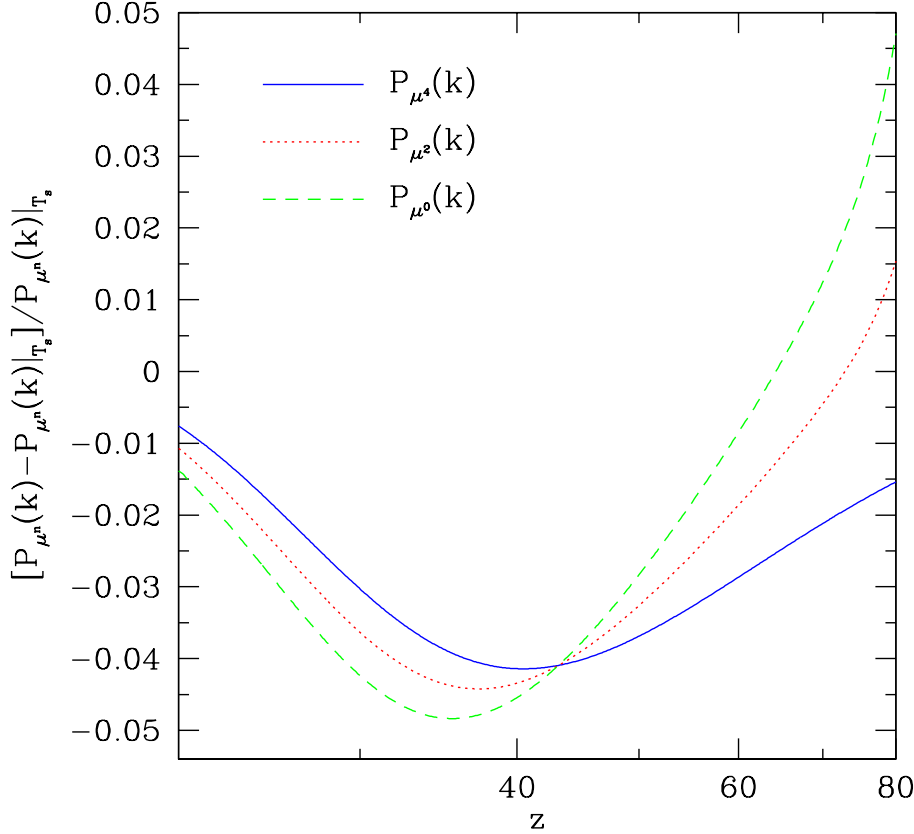


Figure 2. The fractional change in the μ^0 , μ^2 , and μ^4 power spectra resulting from the use of the full distribution function instead of the standard spin temperature formula (Eq. 23 of Madau et al. 1997 with $y_\alpha = 0$) versus redshift.

which is the generalization of the usual definition $T_s = T_*/\ln(3n_0/n_1)$. We can see that the faster-moving atoms have spin temperatures that are closer to the kinetic temperature, which is expected since they undergo more frequent collisions. Conversely, the (more typical) slower-moving atoms nearer to the center of the velocity distribution have spin temperatures that are closer to the CMB temperature. We thus expect the net effect will be a *reduced* magnitude of the 21-cm emissivity.

In Fig. 2, we show how the power spectrum of 21-cm fluctuations on large scales is changed by using kinetic theory in place of the usual assumption of a single spin temperature. These results were determined by examining how $\overline{T_b}$ and $\partial T_b/\partial\delta$ change with the new calculation and then computing (c.f. Eq. 95)

$$\frac{P_{\mu^0}(k)}{P_{\mu^0}(k)|_{T_s}} = \left(\frac{[\partial T_b/\partial\delta]}{[\partial T_b/\partial\delta]|_{T_s}} \right)^2, \quad \frac{P_{\mu^2}(k)}{P_{\mu^2}(k)|_{T_s}} = \frac{[\partial T_b/\partial\delta]}{[\partial T_b/\partial\delta]|_{T_s}} \frac{\overline{T_b}}{\overline{T_b}|_{T_s}}, \quad \text{and} \quad \frac{P_{\mu^4}(k)}{P_{\mu^4}(k)|_{T_s}} = \left(\frac{\overline{T_b}}{\overline{T_b}|_{T_s}} \right)^2. \quad (97)$$

The derivatives with respect to the overdensity δ were calculated assuming the kinetic temperature varies adiabatically, $T_k \propto (1 + \delta)^{2/3}$. As one can see, at the low redshifts $z < 60$ all contributions to the 21-cm signal (μ^0 , μ^2 , and μ^4) are suppressed. At higher redshift, the *fractional* corrections to $P_{\mu^0}(k)$ and $P_{\mu^2}(k)$ become large because $\partial T_b/\partial\delta$ crosses through zero at $z \approx 90$. (The zero-crossing occurs because $\partial T_b/\partial\delta$ contains two effects: one is the increase in collision rate and overall number of hydrogen atoms in overdense regions, which tends to drive T_b to more negative values, while on the other hand the increase in T_k means that if collisions are efficient, T_s and T_b should go up. The former effect dominates at $z < 90$, while the latter effect dominates at $z > 90$; see e.g. Bharadwaj & Ali 2004).

The 21-cm line profile, $\varphi(v)$, is needed if one wishes to consider the smallest-scale fluctuations in the 21-cm radiation. The line profile is a function of the radial velocity and is proportional to the rate of photon emission, i.e. $\varphi(v) \propto \mathcal{N}$ (see Eq. 87). The line profiles for gas at mean density are shown in Fig. 3; here the line profiles have been normalized such that $|\int_{-\infty}^{\infty} \varphi(x) dx| = 1$ (where $x = v/\sigma$). Note that they are wider than Maxwellian, because the fast-moving atoms have a lower spin temperature (i.e. farther from T_γ) than the slow-moving atoms. In Fig. 4 we show the Fourier transform of the line

21-cm line profiles at mean density

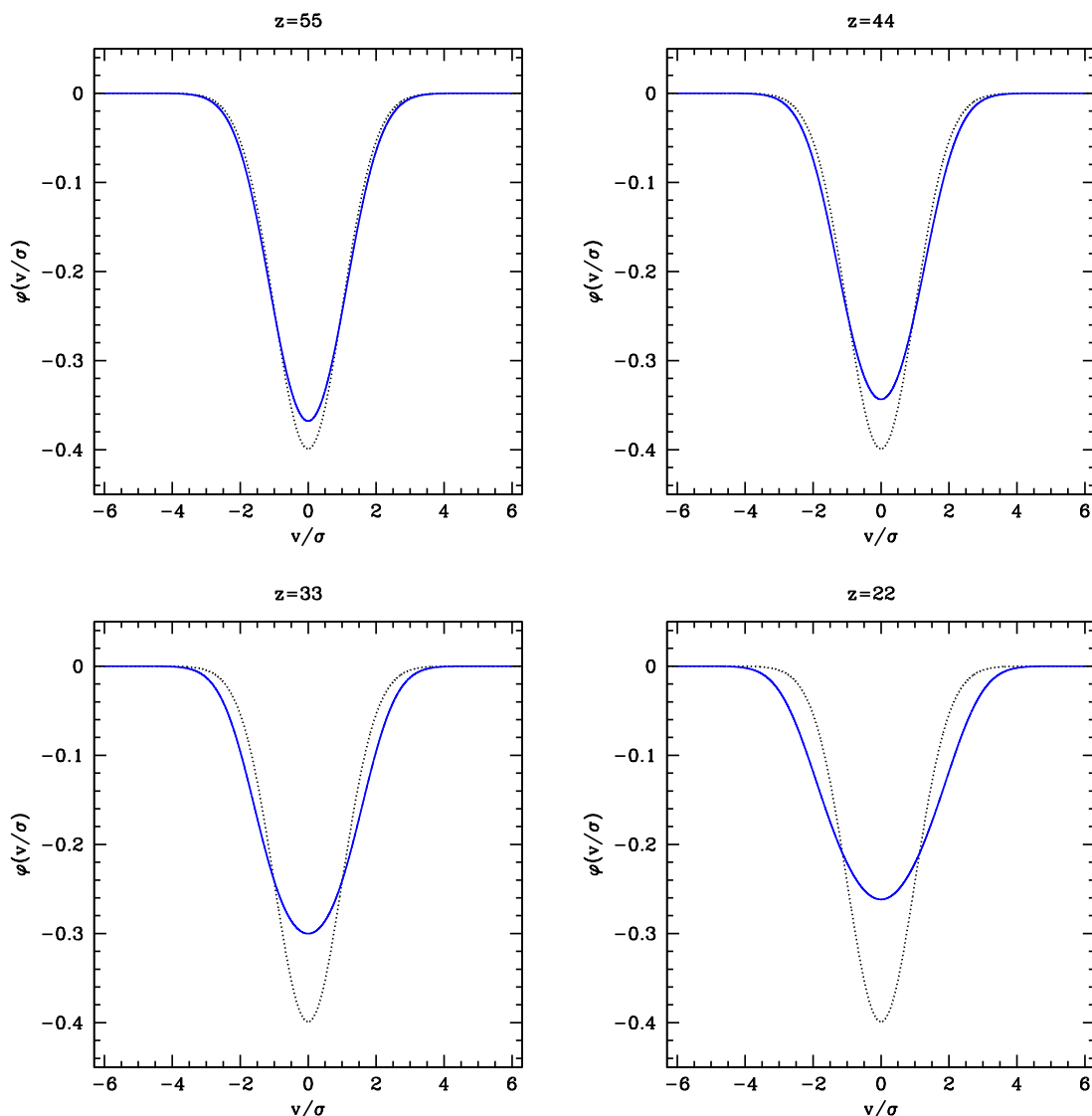


Figure 3. The 21-cm line profile shown for mean density intergalactic gas at several redshifts. The solid (blue) curve is the actual line profile, whereas the dotted (black) curve shows a Maxwellian profile. Note that the profile is significantly wider than Maxwellian, especially at the lower redshifts.

profile, which determines the Doppler cutoff of the 21-cm power spectrum in the radial direction. In the Maxwellian case, the Fourier transform is simply a Gaussian,

$$\frac{\tilde{\varphi}(k)}{\tilde{\varphi}(0)} = e^{-k_{\parallel}^2/2k_T^2}, \quad (98)$$

where $k_T = (1+z)^{-1}H(z)\sigma^{-1}$. Unsurprisingly, the wider-than-Maxwellian line profile in velocity space manifests itself as a cutoff at smaller radial wavenumber k_{\parallel} . This leads to an additional suppression of modes in the 21-cm signal with $|k_{\parallel}|$ greater than a few hundred Mpc^{-1} , which unfortunately makes them even harder to observe. It also means that proposals to measure the IGM temperature using the redshift-space anisotropy caused by the thermal motions of the atoms (Naoz & Barkana 2005) will have to consider in detail the non-Maxwellian nature of the line profile. The widening of the line profile can also be illustrated by plotting the increase in FWHM relative to the Maxwellian case; this is shown in Fig. 5. The line profile for adiabatically compressed gas is shown in Fig. 6. Note that the high-density gas (e.g. in the bottom-right panel with $1+\delta=8$) has a nearly Maxwellian line profile, as expected when collisions dominate over radiative transitions.

Fourier transform of line profile

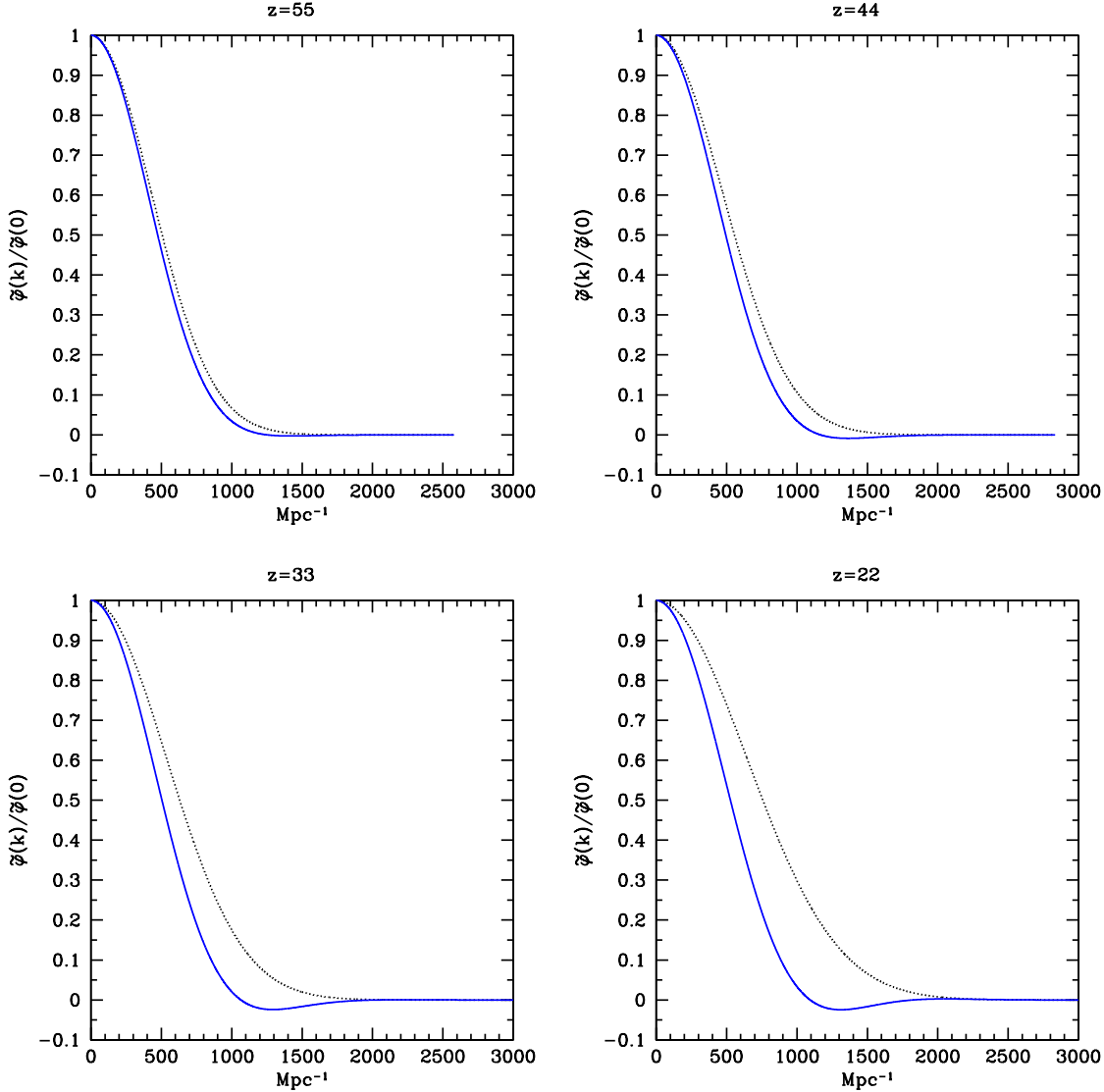


Figure 4. The Fourier transform of the line profile shown for mean density intergalactic gas at several redshifts. The horizontal axis has been converted from the conventional km s^{-1} to the redshift space wavenumber, $k_{\parallel} = (1+z)^{-1}H(z)M_{\parallel}$.

8 DISCUSSION

The redshifted 21-cm radiation from the dark ages is a promising future cosmological probe, and in recent years there has been substantial progress on understanding the theory of this radiation. However in the analyses to date, it has been assumed that the H I atoms can be described by a single spin temperature T_s and a kinetic temperature T_k . We have removed this assumption by describing the gas with a full joint spin-velocity distribution function $f_F(v)$. We find that although the overall (spin-summed) velocity distribution is Maxwellian, the individual velocity distributions of H I in the excited and de-excited hyperfine levels are not. This leads to two effects: a widening of the 21-cm line, i.e. width greater than $\sqrt{k_B T_k / m_H}$; and a suppression of the overall 21-cm signal.

The suppression of the signal on large scales amounts to an effect of up to ~ 5 per cent in the power spectrum. While this is small, it will be essential to consider it if precision cosmological constraints are ever to be obtained from the pre-ionization 21-cm signal (Loeb & Zaldarriaga 2004; Naoz & Barkana 2005). On small scales ($\sim 10^{-2}$ Mpc) the 21-cm line may be broadened up to ~ 1.6 times its Maxwellian width. However, observing these very-small scale features may prove to be even more difficult than the large-scale features since the amount of power per mode is less on small scales, where $P(k) \propto k^{-3}$. An alternative method of identifying small-scale structures is to look at 21-cm absorption features in the spectra of very high-redshift radio sources (Carilli et al. 2002; Furlanetto & Loeb 2002), but it is very unlikely that such sources will

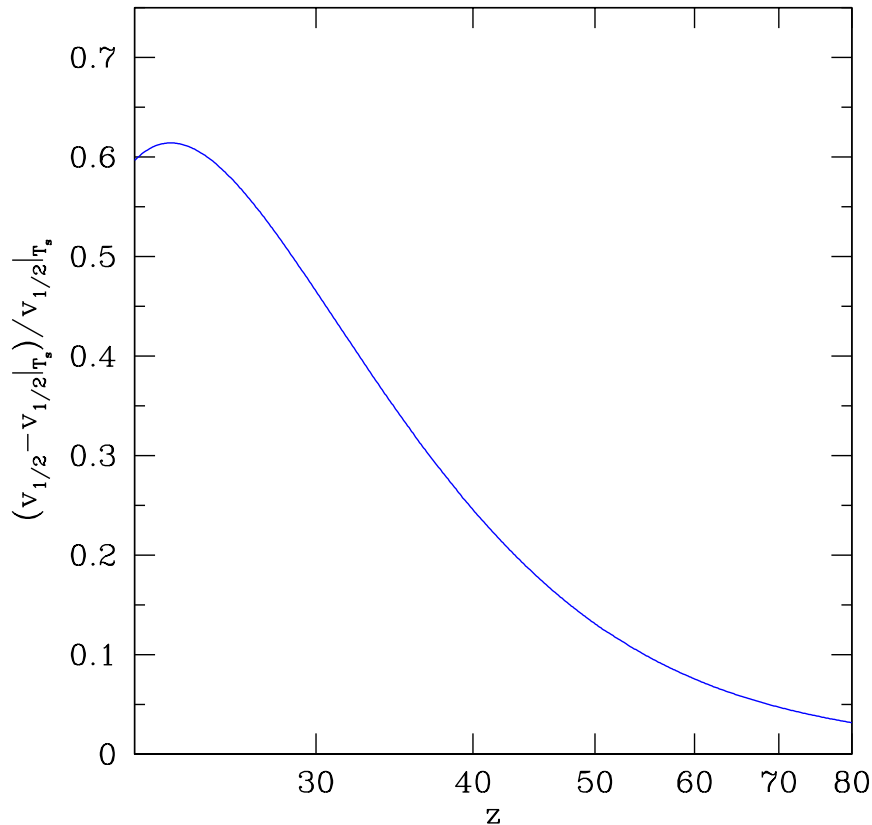


Figure 5. The fractional change in $v_{1/2}$, the velocity at half-maximum of the line profile, as a function of redshift. Note that in the velocity-independent calculation (for a Gaussian line profile) $v_{1/2}|_{T_s} = \sqrt{2 \ln 2} \sigma \simeq 1.18\sigma$.

be found behind a collisionally spin-coupled IGM except in models with unusually early structure formation. Another way that the line profile could be important is in regions such as minihaloes that have significant optical depth (Shapiro et al. 2005), since line self-absorption is suppressed when the line is broadened. In this case the contribution of the minihaloes to the large-scale power spectrum could in principle be detectable even if individual minihaloes are not identified, although even a small amount of Ly α emission could decouple the IGM spin temperature from the CMB and cause the IGM to overwhelm the minihalo signal (Furlanetto & Oh 2006). Note that in the case of a radio source or minihalo, the absorption/emission line profile would be modified since one is no longer seeing the gas against a background at brightness temperature T_γ .

At some point in the evolution of the Universe, UV sources turn on and the IGM temperature is affected by Ly α scattering as well as by collisional and 21-cm transitions (see Furlanetto 2006 for some recent models). A detailed analysis of the spin-velocity distribution in this case is beyond the scope of this paper, although we suspect that the single spin temperature approximation is very good for this case. This is because, at temperatures greater than a few Kelvin and typical IGM Ly α optical depths (of order 10^6), the colour temperature T_c of the Ly α photons relaxes to the gas kinetic temperature, and the width of features in the Ly α spectrum is much wider than the Doppler shift frequency $\sim \nu_{\text{Ly}\alpha} \sigma / c$ induced by the motions of the atoms (Chen & Miralda-Escudé 2004); thus all atoms see a similar Ly α radiation field at similar colour temperature. This circumstance would of course lead to a velocity-independent spin temperature if Ly α and 21-cm dominate over collisions. At temperatures of several Kelvin, obtainable in low-density regions if reionization starts late, the colour temperature can exhibit more complicated behaviour if $T_s \neq T_k$ (Hirata 2006). This could potentially produce a non-Maxwellian line profile and affect the total emissivity; in order to solve this problem one would need to simultaneously solve the radiative transfer and Boltzmann equations for the UV photon spectrum and HI velocity distribution. However the single spin temperature approximation would apply to high accuracy if X-ray heating drives T_k to tens of K or more, or if the Ly α spin-flip scattering rate ever becomes much larger than the 21-cm transition rate (which would thermalize all spins at T_k). Collisions with electrons

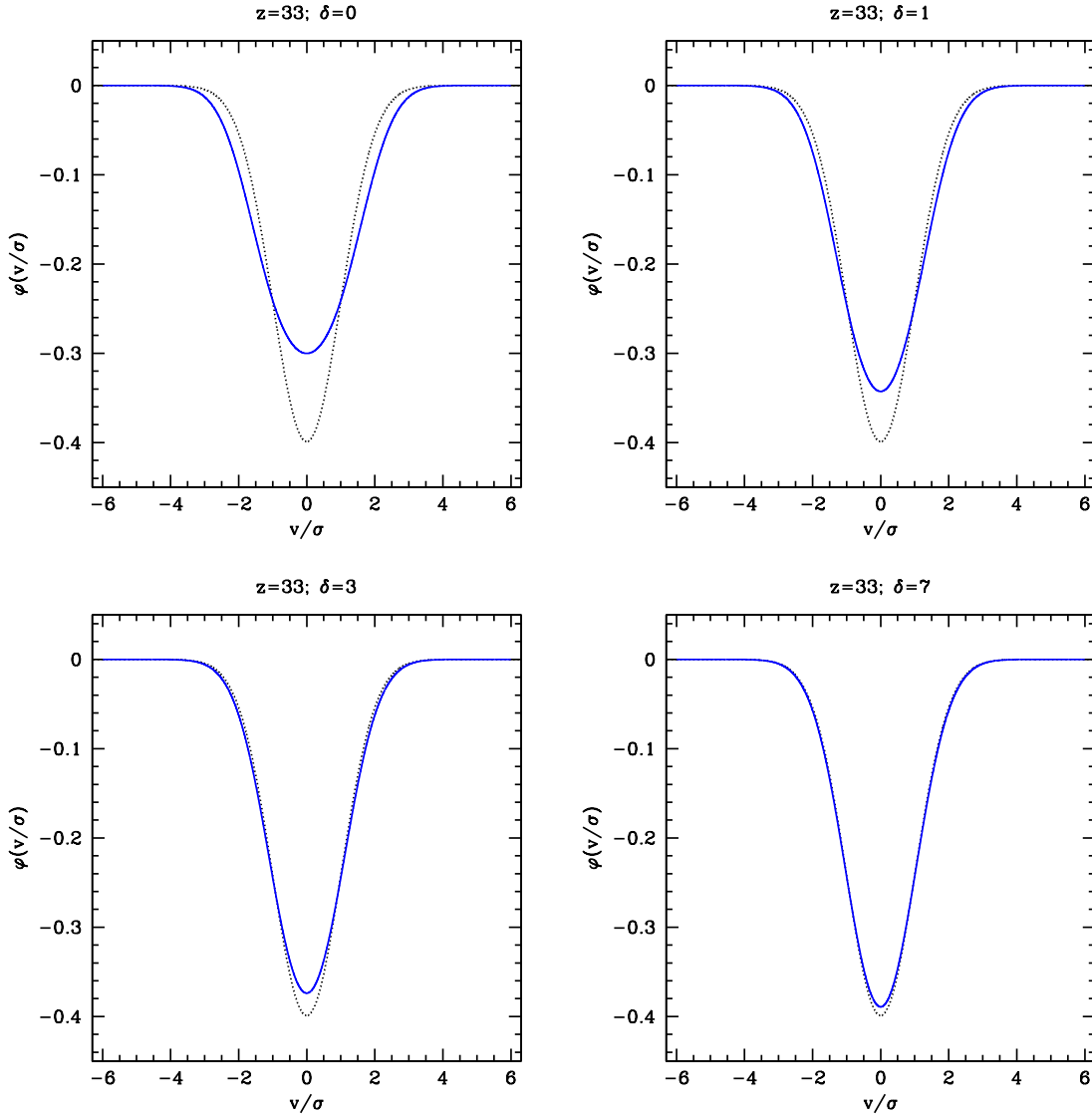
21-cm line profiles at $z=33$ for various overdensities

Figure 6. The 21-cm line profile shown for intergalactic gas at $z = 33$. We show values ranging from mean density ($\delta = 0$, left panel) through 8 times mean density ($\delta = 7$, right panel), assuming a kinetic temperature from adiabatic evolution, $T_k \propto (1 + \delta)^{2/3}$. The solid (blue) curve is the actual line profile, whereas the dotted (black) curve shows a Maxwellian profile. Note that the line profile is more nearly Gaussian at high densities and temperatures where collisions are more effective.

may also be important if there is partial ionization due to X-rays (Kuhlen et al. 2006); this hyperfine transition mechanism is expected to be independent of the atom’s velocity because this is negligible compared to the velocity of the electron.

We conclude that the traditional assumption of a single spin temperature describing the high-redshift gas, while a good first approximation, is incorrect at the several per cent level for the mean signal and at the several tens of per cent level for the line profile. Any calculation aiming for higher precision must thus include the full kinetic theory analysis and the joint spin-velocity distribution of the neutral hydrogen atoms derived here.

ACKNOWLEDGMENTS

We thank S. Furlanetto for insightful comments on a draft of this paper. CH is supported in part by NSF PHY-0503584 and by a grant-in-aid from the W. M. Keck Foundation. KS is supported by NASA through Hubble Fellowship grant HST-HF-01191.01-A awarded by the Space Telescope Science Institute, which is operated by the Association of Universities for Research in Astronomy, Inc., for NASA, under contract NAS 5-26555.

REFERENCES

- Allison A. C., Dalgarno A., 1969, *ApJ*, 158, 423
 Babich D., Loeb A., 2005, *ApJ*, 635, 1
 Barkana R., Loeb A., 2005, *ApJ*, 624, L65
 Bharadwaj S., Ali S., 2004, *MNRAS*, 352, 142
 Bowman J. D., Morales M. F., Hewitt J. N., 2005, preprint (astro-ph/0512262)
 Carilli C. L., Gnedin N. Y., Owen F., 2002, *ApJ*, 577, 22
 Chen X., Miralda-Escudé J., 2004, *ApJ*, 602, 1
 Chuzhoy L., Shapiro P. R., 2005, preprint (astro-ph/0512206)
 Cooray A., Furlanetto S., 2005, *MNRAS*, 359, L47
 Dalgarno A., 1961, *Proc. R. Soc. London A*, 262, 132
 Edmonds A., 1960, *Angular Momentum in Quantum Mechanics* (Princeton: Princeton University Press)
 Field G., 1958, *Proc. I. R. E.*, 46, 240
 Field G., 1959, *ApJ*, 129, 536
 Fixsen D. J., Cheng E. S., Gales J. M., Mather J. C., Shafer R. A., Wright E. L., 1996, *ApJ*, 473, 576
 Frye D., Lie G. C., Clementi E., 1989, *J. Chem. Phys.*, 91, 2366
 Furlanetto S. R., Loeb A., 2002, *ApJ*, 579, 1
 Furlanetto S., 2006, preprint (astro-ph/0604040)
 Furlanetto S., Oh S. P., 2006, preprint (astro-ph/0604080)
 Gradshteyn I. S., Ryzhik I. M., 1994, *Table of integrals, series and products*, 5th. ed. (New York: Academic Press)
 Hirata C. M., 2006, *MNRAS*, 367, 259
 Iliev I. T., Shapiro P. R., Ferrara A., Martel H., 2002, *ApJ*, 572, L123
 Iliev I. T., Scannapieco E., Martel H., Shapiro P. R., 2003, *MNRAS*, 341, 81
 Jamieson M. J., Dalgarno A., Yukich J. N., 1992, *Phys. Rev. A*, 46, 6956
 Jamieson M. J., Dalgarno A., Zygelman B., Krstić, P. S., Schultz D. R., 2000, *Phys. Rev. A*, 61, 014701
 Kolos W., 1967, *Int. J. Quantum Chem.*, 1, 169
 Kolos W., Szalewicz K., Monkhorst H. J., 1986, *J. Chem. Phys.*, 84, 3278
 Kuhlen M., Madau P., 2005, *MNRAS*, 363, 1069
 Kuhlen M., Madau P., Montgomery R., 2006, *ApJ*, 637, L1
 Loeb A., Zaldarriaga M., 2004, *Phys. Rev. Lett.*, 92, 211301
 Madau P., Meiksin A., Rees M., 1997, *ApJ*, 475, 429
 McQuinn M., Zahn O., Zaldarriaga M., Hernquist L., Furlanetto S. R., 2005, preprint (astro-ph/0512263)
 Morales M. F., Bowman J. D., Hewitt J. N., 2005, preprint (astro-ph/0510027)
 Naoz S., Barkana R., 2005, *MNRAS*, 362, 1047
 Pritchard J. R., Furlanetto S. R., 2006, *MNRAS*, 367, 1057
 Santos M. G., Cooray A., Knox L., 2005, *ApJ*, 625, 575
 Seager S., Sasselov D. D., Scott D., 1999, *ApJL*, 523, L1
 Shapiro P. R., Ahn K., Alvarez M. A., Iliev I. T., Martel H., Ryu D., 2005, preprint (astro-ph/0512516)
 Sigurdson K., Furlanetto S. R., 2005, preprint (astro-ph/0505173)
 Smith F. J., *Pl. & Space Sci.*, 1966a, 14, 929
 Smith F. J., *Pl. & Space Sci.*, 1966b, 14, 937
 Tang K. T., Yang X. D., 1990, *Phys. Rev. A*, 42, 311
 Wang X., Tegmark M., Santos M., Knox L., 2005, preprint (astro-ph/0501081)
 Wouthuysen S., 1952, *Astron. J.*, 57, 31
 Zaldarriaga M., Furlanetto S. R., Hernquist L., 2004, *ApJ*, 608, 622
 Zygelman B., Dalgarno A., Jamieson M. J., Stancil P. C., *Phys. Rev. A*, 67, 042715
 Zygelman B., 2005, *ApJ*, 622, 1356

APPENDIX A: PROPERTIES OF THE BASIS FUNCTIONS

Here we summarize some useful properties of the basis functions defined in Eq. (19). These are needed in order to compute the two quantities of observational interest, namely the velocity-marginalized H I level populations $\{n_0, n_1\}$ and the 21-cm line profile (which in general can be non-Gaussian).

Both the level population integrals and the line profile are related to the 3-dimensional Fourier transform of ϕ_n , namely $\tilde{\phi}_n(\mathbf{M}) = \int \phi_n(\mathbf{v}) e^{-i\mathbf{M}\cdot\mathbf{v}} d^3\mathbf{v}$. This quantity can be evaluated by switching to spherical coordinates for \mathbf{v} :

$$\tilde{\phi}_n(\mathbf{M}) = \int \phi_n(\mathbf{v}) e^{-iMv \cos \theta} v^2 \sin \theta \, dv \, d\theta \, d\varphi = 4\pi \int_0^\infty \phi_n(v) \frac{\sin(Mv)}{Mv} v^2 \, dv. \quad (\text{A1})$$

Recalling that $\sigma = \sqrt{k_B T_k / m_H}$, we then have, using Eq. (19),

$$\tilde{\phi}_n(\mathbf{M}) = \frac{2^{-n-1/2} \pi^{-1/2} [(2n+1)!]^{-1/2}}{\sigma^2 M} \int_0^\infty H_{2n+1} \left(\frac{v}{\sigma} \right) e^{-v^2/2\sigma^2} \sin(Mv) \, dv. \quad (\text{A2})$$

We note that H_{2n+1} is odd so the integrand here is even; thus we may replace $\int_0^\infty \rightarrow \frac{1}{2} \int_{-\infty}^\infty$. Also $\sin(Mv) = \Im e^{iMv}$ where \Im denotes imaginary part. If we further substitute $x = v/\sigma$, we get

$$\begin{aligned} \tilde{\phi}_n(\mathbf{M}) &= \frac{2^{-n-3/2} \pi^{-1/2} [(2n+1)!]^{-1/2}}{\sigma M} \Im \int_{-\infty}^\infty H_{2n+1}(x) e^{-x^2/2} e^{iM\sigma x} \, dx \\ &= \frac{2^{-n-1} [(2n+1)!]^{-1/2}}{\sigma M} (-1)^n e^{-\sigma^2 M^2/2} H_{2n+1}(\sigma M), \end{aligned} \quad (\text{A3})$$

where in the second equality we have used the Fourier transform of a product of a Hermite polynomial and a Gaussian (e.g. Eq. 7.376.1 of Gradshteyn & Ryzhik 1994). Using the specific equation for H_{2n+1} , we can see that the integrated line profile is

$$\tilde{\phi}_n(0) = (-1)^n 2^{-n-1} [(2n+1)!]^{-1/2} \lim_{M \rightarrow 0} \frac{H_{2n+1}(\sigma M)}{\sigma M} = (-1)^n 2^{-n-1} [(2n+1)!]^{-1/2} H'_{2n+1}(0) \quad (\text{A4})$$

according to l'Hôpital's rule. The derivative $H'_{2n+1}(0)$ can be determined from the series expansion of H_{2n+1} and gives

$$H'_{2n+1}(0) = (-1)^n \frac{(2n+2)!}{(n+1)!} \rightarrow \tilde{\phi}_n(0) = \frac{\sqrt{(2n+1)!}}{2^n n!}. \quad (\text{A5})$$

In addition to the integrals of the basis modes, provided by Eq. (A5), we also need the contribution of each basis mode to the line profile, defined by

$$\psi_n(v_{\parallel}) = \int \phi_n(\mathbf{v}) \, d^2 \mathbf{v}_{\perp}, \quad (\text{A6})$$

where v_{\parallel} is the component of \mathbf{v} along the line of sight and \mathbf{v}_{\perp} is the component in the plane of the sky. The Fourier transform of the line profile is trivially determined,

$$\begin{aligned} \tilde{\psi}_n(M_{\parallel}) &\equiv \int_{-\infty}^{\infty} \psi_n(v_{\parallel}) e^{iM_{\parallel} v_{\parallel}} \, dv_{\parallel} = \int \phi_n(\mathbf{v}) e^{iM_{\parallel} v_{\parallel}} \, dv_{\parallel} \, d^2 \mathbf{v}_{\perp} = \tilde{\phi}_n(M_{\parallel}) \\ &= \frac{2^{-n-1} [(2n+1)!]^{-1/2}}{\sigma M_{\parallel}} (-1)^n e^{-\sigma^2 M_{\parallel}^2/2} H_{2n+1}(\sigma M_{\parallel}). \end{aligned} \quad (\text{A7})$$

It is in fact this Fourier transform $\tilde{\psi}_n(M_{\parallel})$ that we will need in order to obtain linear theory power spectra. However it is conceptually useful to plot the actual function $\psi_n(v_{\parallel})$, so we calculate this here. It is

$$\psi_n(v_{\parallel}) = \int_0^\infty \phi_n \left(\sqrt{v_{\parallel}^2 + v_{\perp}^2} \right) 2\pi v_{\perp} \, dv_{\perp} = 2\pi \int_{|v_{\parallel}|}^\infty \phi_n(v) v \, dv = 2\pi \int_{v_{\parallel}}^\infty \phi_n(v) v \, dv. \quad (\text{A8})$$

Here the second equality involves the change of variables from v_{\perp} to $v = \sqrt{v_{\parallel}^2 + v_{\perp}^2}$, and the third equality holds because the integrand is odd and hence the integral from v_{\parallel} to $|v_{\parallel}|$ contributes nothing. Plugging in the specific form for the basis modes from Eq. (19) gives

$$\psi_n(v_{\parallel}) = \frac{1}{2\sqrt{2\pi}(2n+1)! \sigma^2} \int_{v_{\parallel}}^\infty H_{2n+1} \left(\frac{v}{\sigma} \right) e^{-v^2/2\sigma^2} \, dv = \frac{1}{2\sqrt{2\pi}(2n+1)! \sigma} \int_{v_{\parallel}/\sigma}^\infty H_{2n+1}(x) e^{-x^2/2} \, dx, \quad (\text{A9})$$

where we have again substituted $x = v/\sigma$. The integral may be solved by using the Hermite polynomial recurrence relations (Eqs. 8.952.1 and 8.952.2 of Gradshteyn & Ryzhik 1994) in the form

$$\begin{aligned} \frac{d}{dx} \left[\frac{1}{2^{2j-1} j!} H_{2j}(x) e^{-x^2/2} \right] &= \frac{1}{2^{2j-1} j!} [H'_{2j}(x) - x H_{2j}(x)] e^{-x^2/2} = \frac{1}{2^{2j-1} j!} \left[2j H_{2j-1}(x) - \frac{1}{2} H_{2j+1}(x) \right] e^{-x^2/2} \\ &= \left[\frac{H_{2j-1}(x)}{2^{2(j-1)} (j-1)!} - \frac{H_{2j+1}(x)}{2^{2j} j!} \right] e^{-x^2/2} \end{aligned} \quad (\text{A10})$$

for $j \geq 1$. In the special case of $j = 0$, it is trivial to see that the same expression is valid if one formally defines $H_{-1}(x)/[(-1)!] = 0$. Summing this equation from $j = 0$ to n , we then get

$$\frac{d}{dx} \left[\sum_{j=0}^n \frac{1}{2^{2j-1} j!} H_{2j}(x) e^{-x^2/2} \right] = -\frac{H_{2n+1}(x)}{2^{2n} n!} e^{-x^2/2}. \quad (\text{A11})$$

With this equation, we can now solve the integral in Eq. (A9),

$$\int_{v_{\parallel}/\sigma}^{\infty} H_{2n+1}(x)e^{-x^2/2} dx = -2^{2n} n! \sum_{j=0}^n \frac{1}{2^{2j-1} j!} H_{2j}(x)e^{-x^2/2} \Big|_{x=v_{\parallel}/\sigma}^{\infty} = \sum_{j=0}^n 2^{2(n-j)+1} \frac{n!}{j!} H_{2j}\left(\frac{v_{\parallel}}{\sigma}\right) e^{-v_{\parallel}^2/2\sigma^2}, \quad (\text{A12})$$

which implies

$$\psi_n(v_{\parallel}) = \frac{1}{\sqrt{2\pi}\sigma} \frac{2^n n!}{\sqrt{(2n+1)!}} \sum_{j=0}^n \frac{H_{2j}(v_{\parallel}/\sigma)}{2^{2j} j!} e^{-v_{\parallel}^2/2\sigma^2}. \quad (\text{A13})$$

This formula is suitable for numerical evaluation and has been used to generate our plots of the 21-cm line profile.

APPENDIX B: CROSS SECTIONS

Derivation of H-H Cross Section

We determine the H-H scattering cross section according to the elastic approximation (Dalgarno 1961). In this approximation we ignore the hyperfine energy defect and treat the collision as a scattering problem with separate potentials $V_0(R)$ and $V_1(R)$ for the electron spin-singlet ($S = 0$) and spin-triplet ($S = 1$) states. The difference between these potentials results in a change in the electronic spin of a particular hydrogen atom, and hence a change in its total (nuclear plus electronic) spin angular momentum. The derivation below is based on the formalism of Smith (1966a,b), although we use the $|SIF_t M_{F_t}\rangle$ basis rather than diagonalizing in S and M_S as was done by Smith (1966a).

There have been many other previous determinations of the cross section for scattering of two hydrogen atoms, some going beyond the elastic approximation; however the published results do not provide the full spin and angular dependence of the cross section, tabulating instead the spin-flip cross section (Allison & Dalgarno 1969; Zygelman et al. 2003; Zygelman 2005) or moments of the angular distribution (Jamieson et al. 1992, 2000).

We are interested in the differential cross section for hydrogen atoms in the F' and F'' hyperfine levels to scatter and leave a hydrogen atom in the F level moving in direction $\hat{\Omega}$. It will be assumed that initially the F'' atom is moving with velocity $w e_3$ relative to the F' atom, so that $\theta = \arccos \hat{\Omega}_3$ is the scattering angle. In our problem the hydrogen spins are unpolarized because the radiation field is isotropic and because in the elastic approximation the atoms cannot be polarized by collisions. Therefore we consider only the cross section summed over final magnetic quantum number M_F and averaged over initial $M_{F'}$ and $M_{F''}$.

We denote the total spin by F_t (the vector sum of F' and F''), and use the labels a and b for the nuclei. The incident wave function of the two hydrogen atoms is then

$$|\Psi_{\text{in}}\rangle = \mathcal{A}_p \mathcal{A}_e \left(|1s_a 1s_b\rangle |F' F'' F_t M_{F_t}\rangle e^{ikZ} \right), \quad (\text{B1})$$

where $(X, Y, Z) = \mathbf{R}_b - \mathbf{R}_a$ is the relative position vector of the two nuclei, $k = m_H w / 2\hbar$ is the wavevector for reduced mass $m_H/2$, $|1s_a 1s_b\rangle$ is the orbital wave function of the two electrons (with $1s_a$ and $1s_b$ representing the $1s$ orbitals associated with nuclei a and b), $|F' F'' F_t M_{F_t}\rangle$ is the spin state of the nuclei a and b and electrons 1 and 2, and $\mathcal{A}_{p,e}$ are the antisymmetrization operators for the protons and electrons. We have chosen our coordinate system such that the relative velocity is along the third coordinate axis. Also the notation $|F_{a1} F_{b2} F_t M_{F_t}\rangle$ refers to the angular momenta $\mathbf{F}_{a1} = \mathbf{I}_a + \mathbf{S}_1$ and $\mathbf{F}_{b2} = \mathbf{I}_b + \mathbf{S}_2$.

The antisymmetrization operators in Eq. (B1) commute with the total electronic and nuclear angular momenta S and I , but not with F_{a1} and F_{b2} . It is thus convenient to re-write Eq. (B1) in the basis of eigenstates of S and I (which we denote $|SI, F_t M_{F_t}\rangle$):

$$\begin{aligned} |\Psi_{\text{in}}\rangle &= \mathcal{A}_p \mathcal{A}_e \left(|1s_a 1s_b\rangle \sum_{S,I} \langle SI, F_t M_{F_t} | F' F'' F_t M_{F_t} \rangle |SI, F_t M_{F_t}\rangle e^{ikZ} \right) \\ &= \frac{1}{2} \sum_{S,I} [|1s_a 1s_b\rangle + (-1)^S |1s_b 1s_a\rangle] \langle SI, F_t M_{F_t} | F' F'' F_t M_{F_t} \rangle |SI, F_t M_{F_t}\rangle [e^{ikZ} + (-1)^{S+I} e^{-ikZ}]. \end{aligned} \quad (\text{B2})$$

The scattered wave function is related to the ingoing wave function by the scattering amplitudes $f(\hat{\Omega})$. These are defined in terms of the large- R asymptotic form for the wave function,

$$|\Psi\rangle \sim e^{ikZ} + \frac{e^{ikR}}{R} f(\hat{\Omega}), \quad (\text{B3})$$

in which an incident state $|\Psi_{\text{in}}\rangle \sim e^{ikZ}$ is mapped into an outgoing scattered state $|\Psi_{\text{scat}}\rangle \sim R^{-1} e^{ikR} f(\hat{\Omega})$. In our case, the ingoing wave function has both singlet and triplet parts with different potentials and hence different scattering amplitudes. Thus we must superpose singlet and triplet solutions in order to obtain the wave function corresponding to Eq. (B2). Since our particles are identical, we must also superpose both the ingoing wave function with e^{ikZ} dependence, and one with e^{-ikZ}

dependence which can be obtained from Eq. (B3) by a parity transformation. Thus the wave function of Eq. (B2) yields an outgoing scattered state

$$|\Psi_{\text{scat}}\rangle = \frac{e^{ikR}}{2R} \sum_{S,I} [|1s_a 1s_b\rangle + (-1)^S |1s_b 1s_a\rangle] \langle SI, F_t M_{F_t} | F' F'' F_t M_{F_t} \rangle |SI, F_t M_{F_t}\rangle [f_S(\hat{\Omega}) + (-1)^{S+I} f_S(-\hat{\Omega})], \quad (\text{B4})$$

where the amplitudes $f_0(\hat{\Omega})$ and $f_1(\hat{\Omega})$ pertain to electron spin singlets and triplets respectively. These scattering amplitudes are determined by solving the Schrödinger equation by the usual partial wave method and we describe the potentials used and other pertinent details at the end of this Appendix.

The differential scattering cross section to put nucleus a and electron 1 into an H atom with total angular momentum F in the final state is then obtained by projecting $|\Psi_{\text{scat}}\rangle$ onto all outgoing states with $F_{a1} = F$ and arbitrary F_{b2} , and then summing the square norms:

$$\begin{aligned} \frac{d\sigma}{d\hat{\Omega}}(F_{a1} = F) &= R^2 \sum_{F_{b2}} |\langle F F_{b2} F_t M_{F_t} | \Psi_{\text{scat}} \rangle|^2 \\ &= \frac{1}{4} \sum_{F_{b2}} \left| \sum_{S,I} \langle SI, F_t M_{F_t} | F' F'' F_t M_{F_t} \rangle \langle F F_{b2} F_t M_{F_t} | SI, F_t M_{F_t} \rangle [f_S(\hat{\Omega}) + (-1)^{S+I} f_S(-\hat{\Omega})] \right|^2. \end{aligned} \quad (\text{B5})$$

(In principle we must also sum over the final values of the F_t and M_{F_t} quantum numbers; however since we have neglected interactions involving the spin these will be conserved and we may simply use their initial values.) To get our final result for the differential cross section for producing a hydrogen atom with total spin F moving in the direction $\hat{\Omega}$, we must average over the initial values of the quantum numbers F_t and M_{F_t} in their statistical ratios, and then multiply by 4 because the final-state hydrogen atom could contain either nucleus (a or b) and either electron (1 or 2). The summation over M_{F_t} is trivial since none of the inner products or amplitudes inside the sum depend on it:

$$\begin{aligned} \sigma_{F'F''} \frac{dP_{F|F'F''}}{d\hat{\Omega}} &= \frac{1}{(2F'+1)(2F''+1)} \sum_{F_t, F_{b2}} (2F_t+1) \left| \sum_{S,I} \langle SI, F_t M_{F_t} | F' F'' F_t M_{F_t} \rangle \langle F F_{b2} F_t M_{F_t} | SI, F_t M_{F_t} \rangle \right. \\ &\quad \left. \times [f_S(\hat{\Omega}) + (-1)^{S+I} f_S(-\hat{\Omega})] \right|^2. \end{aligned} \quad (\text{B6})$$

The evaluation of Eq. (B6) is a straightforward but tedious exercise in angular momentum recoupling theory. The recoupling coefficients $\langle SI, F_t M_{F_t} | F' F'' F_t M_{F_t} \rangle$ are given in terms of the 9- j symbol by

$$\langle SI, F_t M_{F_t} | F' F'' F_t M_{F_t} \rangle = \sqrt{(2S+1)(2I+1)(2F'+1)(2F''+1)} \begin{Bmatrix} 1/2 & 1/2 & S \\ 1/2 & 1/2 & I \\ F' & F'' & F_t \end{Bmatrix} \quad (\text{B7})$$

(Edmonds 1960). Using the specific values of the 9- j symbols, we find

$$\begin{aligned} \sigma_{00} \frac{dP_{0|00}}{d\hat{\Omega}} &= \frac{1}{16} |f_{00}(\hat{\Omega}) + 3f_{11}(\hat{\Omega})|^2, \\ \sigma_{00} \frac{dP_{1|00}}{d\hat{\Omega}} &= \frac{3}{16} |f_{00}(\hat{\Omega}) - f_{11}(\hat{\Omega})|^2, \\ \sigma_{01} \frac{dP_{0|01}}{d\hat{\Omega}} &= \frac{1}{16} |f_{01}(\hat{\Omega}) + f_{10}(\hat{\Omega}) + 2f_{11}(\hat{\Omega})|^2, \\ \sigma_{01} \frac{dP_{1|01}}{d\hat{\Omega}} &= \frac{1}{16} |f_{01}(\hat{\Omega}) + f_{10}(\hat{\Omega}) - 2f_{11}(\hat{\Omega})|^2 + \frac{1}{8} |f_{01}(\hat{\Omega}) - f_{10}(\hat{\Omega})|^2, \\ \sigma_{10} \frac{dP_{0|10}}{d\hat{\Omega}} &= \frac{1}{16} |f_{01}(\hat{\Omega}) + f_{10}(\hat{\Omega}) - 2f_{11}(\hat{\Omega})|^2, \\ \sigma_{10} \frac{dP_{1|10}}{d\hat{\Omega}} &= \frac{1}{16} |f_{01}(\hat{\Omega}) + f_{10}(\hat{\Omega}) + 2f_{11}(\hat{\Omega})|^2 + \frac{1}{8} |f_{01}(\hat{\Omega}) - f_{10}(\hat{\Omega})|^2, \\ \sigma_{11} \frac{dP_{0|11}}{d\hat{\Omega}} &= \frac{1}{48} |f_{00}(\hat{\Omega}) - f_{11}(\hat{\Omega})|^2 + \frac{1}{24} |f_{01}(\hat{\Omega}) - f_{10}(\hat{\Omega})|^2, \quad \text{and} \\ \sigma_{11} \frac{dP_{1|11}}{d\hat{\Omega}} &= \frac{1}{144} |3f_{00}(\hat{\Omega}) + f_{11}(\hat{\Omega})|^2 + \frac{1}{24} |f_{01}(\hat{\Omega}) - f_{10}(\hat{\Omega})|^2 + \frac{1}{12} |f_{01}(\hat{\Omega}) + f_{10}(\hat{\Omega})|^2 + \frac{5}{9} |f_{11}(\hat{\Omega})|^2, \end{aligned} \quad (\text{B8})$$

where $f_{SI}(\hat{\Omega}) = f_S(\hat{\Omega}) + (-1)^{S+I} f_S(-\hat{\Omega})$.

Derivation of He-H Cross Section

The He-H cross section is actually simpler to derive than H-H because the He atom has no electronic spin or orbital angular momentum. Thus there is only one relevant electronic state, $X^2\Sigma^+$, and there is no spin exchange. The scattering cross section is independent of spin and given by the usual formula, $d\sigma/d\hat{\Omega} = |f(\hat{\Omega})|^2$, where $f(\hat{\Omega})$ is the scattering amplitude in the $X^2\Sigma^+$ potential.

Potentials, Phase Shifts and Scattering Amplitudes

In order to calculate the cross sections as outlined above we must calculate the scattering amplitude $f(\hat{\Omega})$ in the atomic potential $V(R)$. To do this we solve the Schrödinger equation

$$-\frac{\hbar^2}{2\mu}\nabla^2\Psi + (V - E)\Psi = 0, \quad (\text{B9})$$

where $\Psi = \langle \mathbf{R} | \Psi \rangle$, μ is the reduced mass of the two colliding atoms, and $E = \hbar^2 k^2 / 2\mu$ for an unbound state with wavevector \mathbf{k} . For a spherically symmetric potential the wavefunction can be expanded in a basis of angular momentum eigenfunctions as

$$\Psi(R, \hat{\Omega}) = \sum_{N=0}^{\infty} \frac{a_N}{R} \psi_N(R) P_N(\hat{\mathbf{k}} \cdot \hat{\Omega}) \quad (\text{B10})$$

where N is the orbital angular momentum quantum number, the a_N are constant coefficients, P_N are Legendre polynomials, and the partial wave ψ_N satisfies the radial equation

$$\frac{d^2\psi_N}{dR^2} + \left[k^2 - \frac{N(N+1)}{R^2} - \frac{2\mu}{\hbar^2} V(R) \right] \psi_N = 0. \quad (\text{B11})$$

For $R > \mathcal{R}$, where $V(\mathcal{R}) \ll E - N(N+1)\hbar^2/(2\mu\mathcal{R}^2)$, ψ_N takes the approximate form (exact for $R \rightarrow \infty$ or $V \rightarrow 0$)

$$\psi_N \simeq \mathcal{S}_N(kR) \cos \delta_N + \mathcal{C}_N(kR) \sin \delta_N \quad (\text{B12})$$

where δ_N is the phase shift of the N^{th} partial wave, and $\mathcal{S}_N(kR)$ and $\mathcal{C}_N(kR)$ are Riccati-Bessel functions, which are related to the spherical Bessel and spherical Neumann functions by $\mathcal{S}_N(x) = x j_N(x)$ and $\mathcal{C}_N(x) = -x n_N(x)$. Using Eq. (B12) and the asymptotic forms

$$\lim_{R \rightarrow \infty} \mathcal{S}_N(kR) \rightarrow \sin\left(kR - \frac{N\pi}{2}\right) \quad \text{and} \quad \lim_{R \rightarrow \infty} \mathcal{C}_N(kR) \rightarrow \cos\left(kR - \frac{N\pi}{2}\right), \quad (\text{B13})$$

it is straightforward to prove the *exact* integral identities

$$\sin \delta_N = -\frac{2\mu}{\hbar^2} \int_0^{\infty} V(R) \psi_N(R) \mathcal{S}_N(kR) dR, \quad (\text{B14})$$

and

$$\cos \delta_N = \frac{2\mu}{\hbar^2} \int_0^{\infty} \left(V(R) + \frac{2N}{R^2} \right) \psi_N(R) \mathcal{S}_{N-1}(kR) dR. \quad (\text{B15})$$

We use these integral forms to solve for $\delta_N = \delta_N(k)$ while simultaneously solving Eq. (B11) for $\psi_N(R)$. Given these phase shifts the scattering amplitude,

$$f(\hat{\Omega}) = \frac{1}{k} \sum_{N=0}^{\infty} (2N+1) e^{i\delta_N} \sin \delta_N P_N(\hat{\mathbf{k}} \cdot \hat{\Omega}), \quad (\text{B16})$$

can immediately be found.

For this calculation we needed the scattering amplitude in the singlet $X^1\Sigma_g^+$ and triplet $b^3\Sigma_u^+$ potentials for H-H scattering, and in the He-H $X^2\Sigma^+$ scattering potential. We used the same H-H potentials used in Sigurdson & Furlanetto (2005), which is a combination of several previously published H_2 surfaces, interpolations, and asymptotic formulas (Kolos 1967; Kolos et al. 1986; Frye et al. 1989; Jamieson et al. 1992). For the He-H potential, we used the fitting formula by Tang & Yang (1990).